Simple thermodynamics for unravelling sophisticated self-assembly processes

Josef Hamacek, Michal Borkovec and Claude Piguet*

Received 3rd January 2006, Accepted 14th February 2006
First published as an Advance Article on the web 1st March 2006
DOI: 10.1039/b518461d

During the past 15 years, coordination chemistry has rapidly developed toward multicomponent assemblies involving several ligands and metal ions, which are connected *via* intra- or intermolecular processes. The fascinating structural aspect of these complexation reactions has been early recognized for the design of sophisticated (supra)molecular architectures with novel topologies and functions, while the concomitant energetic part only recently emerged as a potential tools for controlling and programming self-assemblies. In this Perspective, we focus on the modelling of the free energy changes accompanying self-assembly processes. Starting with the original protein-ligand model borrowed from biology, which describes complicated multicomponent assemblies, we present (i) its adaptation to coordination chemistry and (ii) its significance for addressing cooperativity as an extra energy cost resulting from intercomponent interactions. An additional entropic concept arising from the separation of intra- and intermolecular complexation processes is then discussed, together with its explicit consideration for modeling multicomponent complexation reactions. Finally, both aspects (*i.e.* cooperativity and intra-/intermolecular connections) are combined in the extended site binding model, which is able to dissect free energy changes occurring in sophisticated metal–ligand assemblies with a minimum set of microscopic parameters. Applications to experimental complexation reactions of increasing complexity are systematically discussed, and illustrate the potential and limitations of each model.

1 Self-assembly in coordination chemistry: semantics, architectures and energetics

Up to 1987, and the publication of the first double-stranded trimetallic helicate $[Cu_3(L1)_2]^{3+}$ by Lehn and co-workers (Fig. 1),[1] research in coordination chemistry mainly focussed on 'standard' complexation reactions involving one metal ion and several ligands. The subsequent and rapid growth of metallosupramolecular chemistry, which aims at preparing sophisticated polymetallic oligomers based on various intercomponent interactions (dative bonds, dispersion forces, hydrogen bonds, *etc*···) has considerably transformed this field.[2]

The resulting complicated and aesthetically appealing complexes represented a strong driving force for rationalizing their formation (Fig. 2), and remarkable qualitative predicting tools rapidly emerged, which are based on (i) the matching between the stereochemical preferences of the metal ions and the ligand binding possibilities,[3] (sometimes referred to as incommensurate symmetry interactions,[2g,4] or interactional algorithms[5]), (ii) the maximum occupancy of the binding sites[5] and (iii) the combination of geometrical shapes in crystals and macroscopic edifices.[6]

The systematic design of novel synthetic strategies, in which the dominant thermodynamic control was sometimes combined with kinetic restrictions for preparing (supra)molecular architectures, was considered as a reminiscence of the edifices produced in living cells, which are built from convergent assemblies of smaller subunits.[7] This similitude between advanced coordination chemistry and biologically relevant processes was first mentioned by

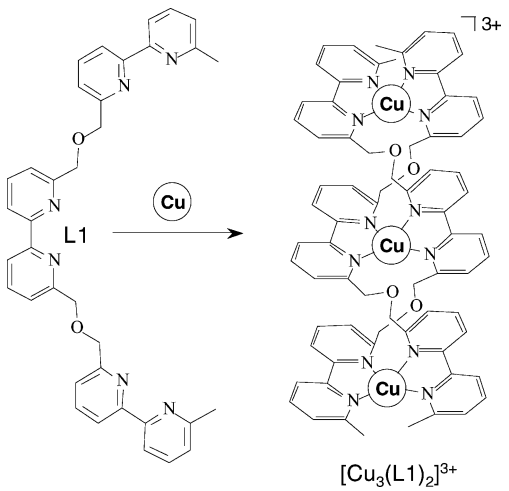

Fig. 1 Self-assembly of the trimetallic double-stranded helicate $[Cu_3(L1)_2]^{3+}$.[1]

Lehn and co-workers in 1987 when reporting on the formation of $[Cu_3(L1)_2]^{3+}$ (Fig. 1), which '*opens ways to the design and study of self-assembling systems presenting cooperativity and regulation features*'.[1] The subsequent use of a novel semantics such as self-organization,[8] self-recognition,[5a] self-healing[9] and self-resolution,[9] combined with unfamiliar terms in coordination chemistry (cooperativity, allostery, algorithm, subroutine) promotes in the rapid recognition of these multivalent processes as part of a new emerging field.[10] In fifteen years, the term self-assembly, which indeed corresponds to the spontaneous formation of higher-ordered structures from molecular building blocks, often held together by weak non-covalent interactions, has become one of the core concepts of supramolecular chemistry.[11] In order

Department of Inorganic, Analytical and Applied Chemistry, University of Geneva, 30 quai Ernest Ansermet, CH-1211, Geneva 4. E-mail: Claude.Piguet@chiam.unige.ch; Fax: (41 22) 379 6830; Tel: (41 22) 379 6034

Josef Hamacek obtained his PhD from Masaryk University, Brno (Czech Republic), under the supervision of Professor Josef Havel in the field of capillary electrophoresis. He pursued his formation as a Marie Curie postdoctoral fellow in the group of Dr Anne-Marie Albrecht-Gary at the University Louis Pasteur, Strasbourg, where his research work was focused on the kinetic and thermodynamic studies of self-assembly processes. In 2003 he joined the group of Professor Claude Piguet at the University of Geneva as a post-doctoral co-worker. Present research interests include the characterisation of supramolecular lanthanide complexes in solution and the development of predictive thermodynamic models.

Michal Borkovec is currently chairman and full professor at the Department of Inorganic, Analytical and Applied Chemistry, University of Geneva. He received his PhD 1986 in Chemical Physics at Columbia University, New York, and until 1998 was active as a lecturer at Swiss Federal Institute of Technology (ETH) Zürich, Switzerland, and until 2001 as professor at Clarkson University, Potsdam, New York. His research interests are physical and analytical chemistry of reaction mechanisms of ion binding, structure and properties of dispersions containing colloidal particles and polymers, and application of this research in the industry and environment. He has coauthored more than 130 scientific articles, and in 2001 received the Raphael Eduard Liesegang Prize of the German Colloid Society.

Claude Piguet earned a PhD degree in 1989 from the University of Geneva in the field of biomimetic copper–dioxygen complexes. After postdoctoral periods in the groups of Professors J.-M. Lehn, A. F. Williams and J.-C. G. Bünzli, he initiated research projects in the field of the lanthanide supramolecular chemistry. In 1995 he received the Werner Medal of the New Swiss Chemical Society and was appointed in 1999 as full professor of inorganic chemistry at the University of Geneva. He has coauthored more than 120 scientific articles in various fields of chemistry, which include the design of discrete multimetallic supramolecular edifices and the unravelling of the thermodynamic origin of their self-assembly processes, the programming of novel electronic functions depending on intermetallic communications, the molecular tuning of local dielectric constants, the preparation of lanthanide-containing metallomesogens and the development of paramagnetic NMR methods for addressing solution structures.

Josef Hamacek

Michal Borkovec

Claude Piguet

to create unambiguous links between metallosupramolecular and biological assemblies, Lindsey introduced a wide-ranging classification scheme, in which seven different classes of self-assembly processes could be recognized, each being further divided into four additional categories depending on the nature of the intercomponent interactions (covalent or non-covalent), and on their origins (biological or abiotic).[12] As far as synthetic coordination complexes are concerned, the usual thermodynamically controlled complexation processes refer to strict self-assembly (class 1). The special case of kinetically controlled complexation processes occurring with poorly labile transition metal ions (Cr^{III}, Ru^{II}, Os^{II}, Pd^{II}, Pt^{II}) corresponds to irreversible self-assembly (class 2). Finally, template reactions, in which one cation (or anion) is used for the thermodynamic (pre)organization of the components, prior to some final transformations leading to kinetically inert edifices, are part of self-assembly with post-modification (class 4). However, this terminology does not take into account the fundamental symmetry rules, which have been early recognized as crucial parameters for predicting the structures of the final multicomponent architectures.[2–4] In an attempt to reliably classify self-assembled metal-containing molecular polyhedra and polygons according to symmetry rules, Stang and co-workers[13] proposed a terminology based on two descriptors **L** and **A**, which respectively stand for **L**inear and **A**ngular rigid building blocks. The assembly is then described by subscripting the number and superscripting the topicity of each involved building block. However, some self-assembly processes escaped a unique description with this method and Swiegers and co-workers completed this notation by using lower case **d** or **a** to indicate whether the binding site is donor or acceptor.[14] Therefore, the final structures in complicated assembly processes can be easily recognized and compared with other sophisticated architectures (Fig. 3).

This efficient structural description combined with the incredible diversity in the structures of metallosupramolecular complexes reported during the last two decades fully justify the use of this novel semantics for extending classical coordination concepts.[2] Conversely, the energetic description of the self-assembly processes remained archaic and poorly understood. In 1992, Lehn and co-workers reported on the thermodynamic equilibria (1)–(4), which

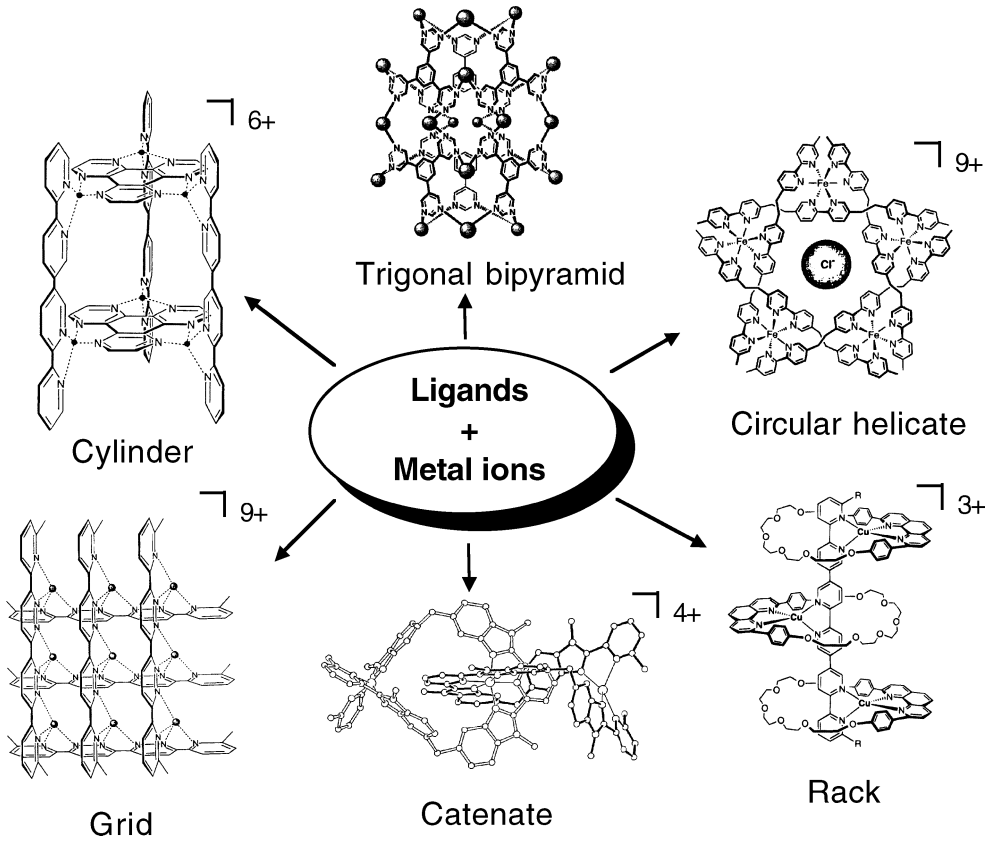

Fig. 2 Selected metallosupramolecular complexes obtained by self-assembly. Reproduced with permission from ref. 23, © Elsevier Science, 2005.

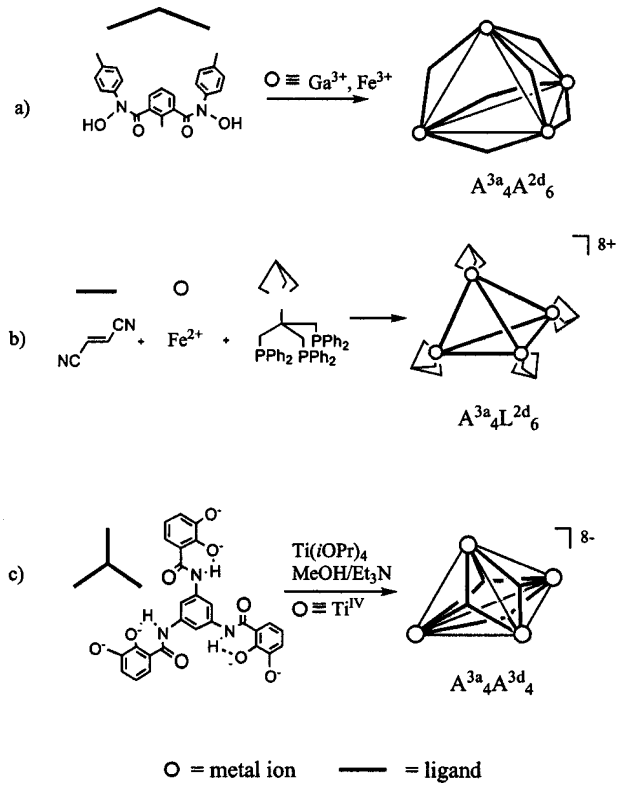

Fig. 3 Abbreviations of some sophisticated self-assembled structures according to the Stang–Swiegers notation. Reproduced with permission from ref. 14. © Wiley-VCH, 2001.

led to the self-assembly of the trimetallic double-stranded helicate $[Cu_3(L2)_2]^{3+}$ (see Scheme 1 for the structure of the ligand).[15]

$$Cu^+ + L2 \rightleftharpoons [Cu(L2)]^+ : \log(\beta_{11}^{Cu,L2}) = 4.6 \quad (1)$$

$$Cu^+ + 2\,L2 \rightleftharpoons [Cu(L2)_2]^+ : \log(\beta_{12}^{Cu,L2}) = 8.2 \quad (2)$$

$$2\,Cu^+ + 2\,L2 \rightleftharpoons [Cu_2(L2)_2]^{2+} : \log(\beta_{22}^{Cu,L2}) = 13.5 \quad (3)$$

$$3\,Cu^+ + 2\,L2 \rightleftharpoons [Cu_3(L2)_2]^{3+} : \log(\beta_{32}^{Cu,L2}) = 18.6 \quad (4)$$

Assuming that the thermodynamic protein-ligand model[16] is adequate for the description of this assembly process, simple graphical tests for cooperativity (Hill plots[17] and Scatchard plots[18]) suggest that the formation of the final trimetallic helicate $[Cu_3(L2)_2]^{3+}$ is driven to completion by positive cooperativity as evidenced by a concave Scatchard plot (Fig. 4(a)), despite the expected electrostatic repulsion operating between cations separated by 5.8 Å.[15] This surprising attractive interaction, which is able to invert electrostatic trend, has been taken for a decade as an additional justification for considering multicomponent metal–ligand complexation reactions as rather different from the classical coordination of ligands to a single metal ion, which is generally characterized by negative cooperativity.[19]

In 2003, the related assemblies of the trimetallic lanthanide triple-stranded helicates $[Ln_3(L3)_3]^{9+}$, shown in equilibria (5)–(7), similarly provide concave Scatchard plots (Fig. 4(b)) assigned to positive cooperativity, despite the alignment of three triply charged cations separated by 9 Å in the final helicates.[20] A few months later,

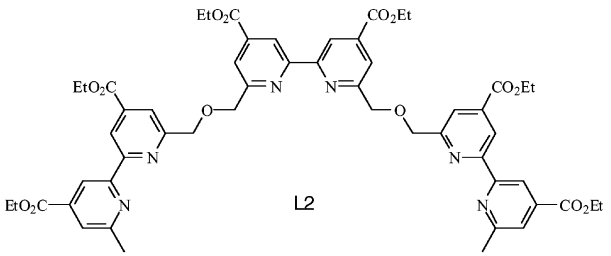

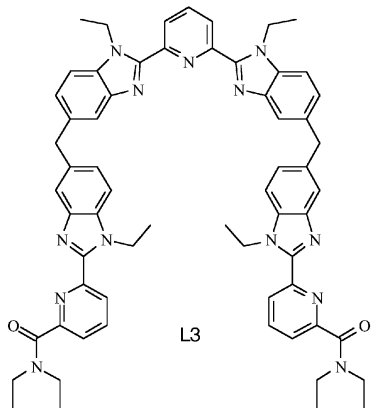

Scheme 1 Structures of the ligands L2 and L3.

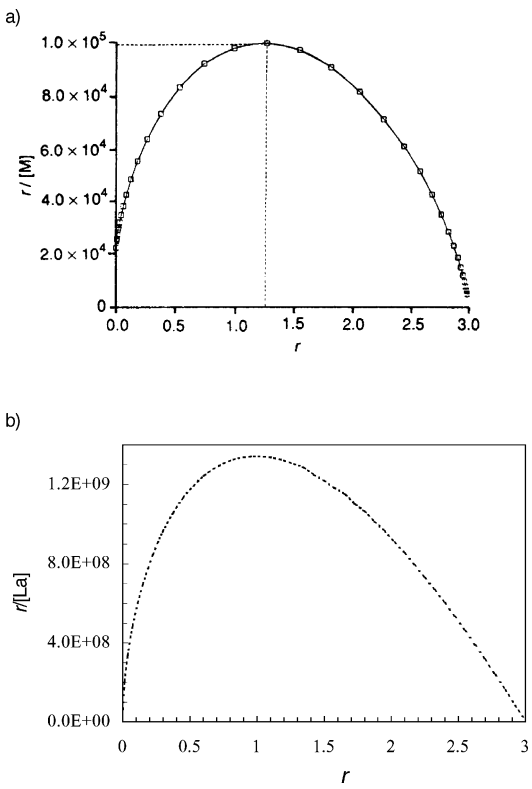

Fig. 4 (a) Concave Scatchard plot for the formation of the double-stranded helicate $[Cu_3(L2)_2]^{3+}$.[15] Reproduced with permission from ref. 15, © Royal Society of Chemistry, 1992. (b) Concave Scatchard plot for the formation of the triple-stranded helicate $[La_3(L3)_3]^{9+}$.[20] Reproduced with permission from ref. 20, © Wiley–VCH, 2003.

Ercolani judiciously pointed out that these assemblies (equilibria (1)–(7)) combine inter- and intramolecular connections between the components, a situation which cannot be accounted for by using the protein-ligand model, and the associated Scatchard plots because the latter approach is strictly limited to successive intermolecular complexation processes.[21]

$$2\,Ln^{3+} + 3\,L3 \rightleftharpoons [Ln_2(L3)_3]^{6+}: \log(\beta_{23}^{Ln,L3}) \quad (5)$$

$$3\,Ln^{3+} + 3\,L3 \rightleftharpoons [Ln_3(L3)_3]^{9+}: \log(\beta_{33}^{Ln,L3}) \quad (6)$$

$$3\,Ln^{3+} + 2\,L3 \rightleftharpoons [Ln_3(L3)_2]^{9+}: \log(\beta_{32}^{Ln,L3}) \quad (7)$$

This seminal article[21] resulted in a revival of interest for reliably dissecting the various free energy contributions to multivalent self-assembly processes. Beyond the principle of maximum site occupancy, which favors the formation of saturated complexes with respect to unsaturated ones,[5] the systematic formation of a maximum number of small symmetrical saturated oligomers, instead of longer polymeric edifices (Fig. 5),[5,22] can be rationalized by the combination of converging enthalpic and entropic driving forces.

Let us consider the assembly of eight components to form either two cyclic tetramers (path (a) in Fig. 6), a single cyclic octamer (path (b) in Fig. 6) or a linear octamer (path (c) in Fig. 6). In absence of solvent effects, the enthalpic contribution can be estimated by calculating the number of intercomponent connections per building block in the final assemblies. For discrete cyclic structures made up of n components (pathways (a) and (b)), we easily recognize that the number of intercomponent connections is equal to the number of components, and thus the average number of intercomponents interactions per subunit is $n/n = 1$. For the related linear structure (pathway (c)), we calculate that the average connection per subunit is $(n - 1)/n = 7/8 = 0.875$. This modest enthalpic preference for cyclic structures obviously decreases with an increased number of components, and it can be easily balanced (and even inverted) by secondary intramolecular effects resulting from ring strains. Therefore, the preference for the formation of a set a small oligomers can be ascribed to the loss in translational entropy accompanying the formation of a single polymer, even if the magnitude of this trend can be modulated by the conformational entropies characterizing smaller oligomers.[7,11,19] The formation of two tetramers in Fig. 6 is thus entropically favored over the formation of a single octamer.

In metallosupramolecular chemistry, the latter entropic consideration usually justifies the formation of a maximum number of well-defined complexes as shown in Fig. 5. This aspect can be strengthened by a judicious tuning of the relative stoichiometries and total concentrations of the metals and ligands.[3,22] Moreover, the concomitant application of the enthalpic principle of maximum site occupancy[5] involves the formation of a maximum of dative bonds, in line with a good matching between the metal ion stereochemical preferences and the ligand binding possibilities. It is worth stressing that we neglect solvation processes in this rough thermodynamic analysis, but the latter effects are crucial and provide complicated, and often opposite, enthalpic and entropic

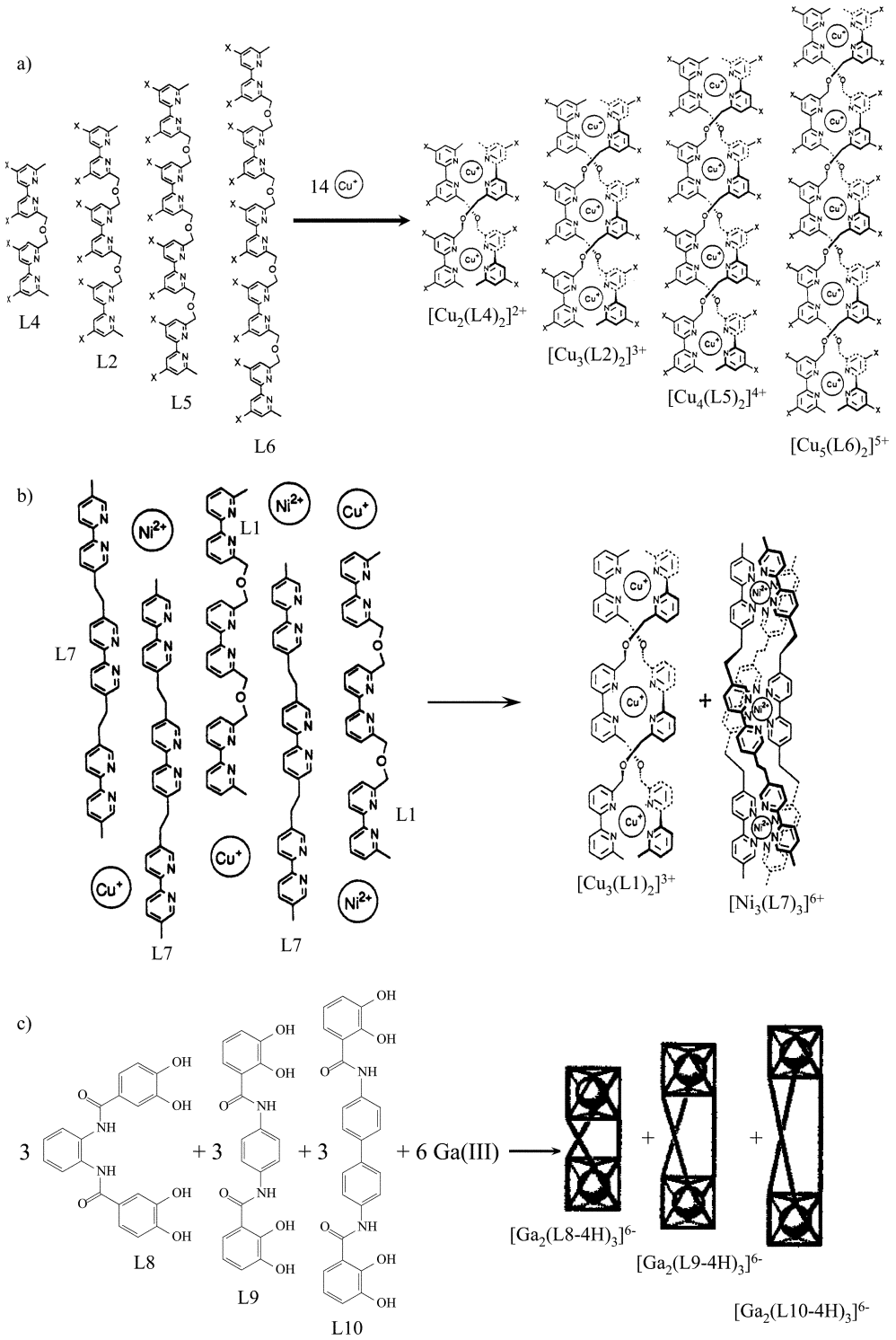

Fig. 5 Self-recognition of (a) homopolymetallic double-stranded helicates $[Cu_m(Ln)_2]^{m+}$,[5a] (b) multiple-stranded helicates $[Cu_3(L1)_2]^{3+}$ and $[Ni_3(L7)_3]^{6+}$,[5a] and (c) homoleptic triple-stranded helicates $[Ga_2(Ln-4H)_3]^{6-}$.[22]

contributions. We thus realize that modelling the energetics in polymetallic complexes represents a difficult challenge, and its current level of rationalization is limited to free energy changes (ΔG), which combine enthalpic and entropic contributions.[21,23] In this Perspective, we present a didactic introduction to the three models, which have been developed for rationalizing the free energy changes (and associated thermodynamic stability) related to the self-assembly of polymetallic complexes. The theoretical treatment will be kept at the simplest level compatible with a rigorous description of the thermodynamic equilibria. Correlations with standard complexation processes reminiscent to coordination chemistry are especially highlighted.

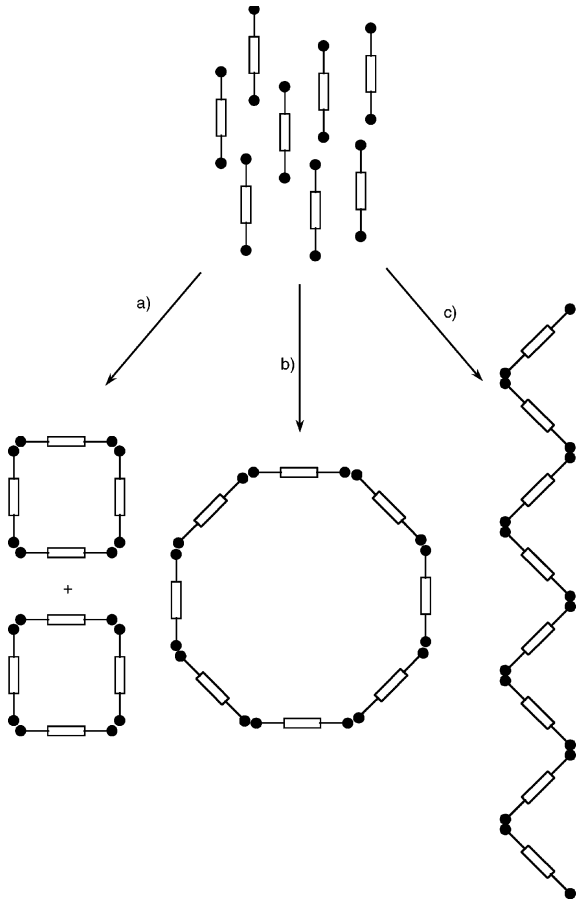

Fig. 6 Assembly of eight components leading to (a) two cyclic tetramers, (b) a cyclic octamer and (c) a linear octamer.

2 Modeling strictly intermolecular complexation processes: the site binding model

The successive complexation of n ligands L to a single metal ion M according to equilibria (8)–(11) indeed corresponds to strictly intermolecular processes, typical of the formation of standard coordination complexes (each ligand is considered as being attached by a single connecting point to M).

$$\mathrm{M} + \mathrm{L} \rightleftharpoons [\mathrm{ML}]\text{: } K_1^{\mathrm{M,L}} \tag{8}$$

$$\mathrm{ML} + \mathrm{L} \rightleftharpoons [\mathrm{ML_2}]\text{: } K_2^{\mathrm{M,L}} \tag{9}$$

$$\mathrm{ML_{(}}_{i-1)} + \mathrm{L} \rightleftharpoons [\mathrm{ML}_i]\text{: } K_i^{\mathrm{M,L}} \tag{10}$$

$$\mathrm{ML_{(}}_{n-1)} + \mathrm{L} \rightleftharpoons [\mathrm{ML}_n]\text{: } K_n^{\mathrm{M,L}} \tag{11}$$

The associated cumulative stability constants $\beta_{1i}^{\mathrm{M,L}} = \prod_{k=1}^{i} K_k^{\mathrm{M,L}}$ can be simply expressed by dissecting the total free energy change $\Delta G_{1i}^{\mathrm{M,L}}$ into (a) i free energies of intermolecular connection $\Delta G_{\mathrm{connection}}^{\mathrm{M,L}} = -RT\ln(k^{\mathrm{M,L}})$, whereby $k^{\mathrm{M,L}}$ is the microscopic affinity for a single M–L connection, and (b) a statistical contribution $\Delta G_{\mathrm{deg}}^{\mathrm{M,L}} = -RT\ln(\Omega_i^{\mathrm{M,L}})$, whereby $\Omega_i^{\mathrm{M,L}}$ stands for the number of microstates contributing to the macrospecies (eqn (12)). According to a pure statistical description of the complexation process, $\Omega_i^{\mathrm{M,L}}$ corresponds to the number of possible arrangement of i ligands among n equivalent binding sites on the metal, and is given by the binomial coefficient $\Omega_i^{\mathrm{M,L}} = C_i^n = n!/((n-i)!i!)$.

$$\begin{aligned}\Delta G_{1i}^{\mathrm{M,L}} &= -RT\ln(\beta_{1i}^{\mathrm{M,L}}) = i\Delta G_{\mathrm{connection}}^{\mathrm{M,L}} + \Delta G_{\mathrm{deg}}^{\mathrm{M,L}} \\ &= -iRT\ln(k^{\mathrm{M,L}}) - RT\ln(\Omega_i^{\mathrm{M,L}})\end{aligned} \tag{12}$$

In the absence of interligand interactions, straightforward algebra transforms eqn (12) into eqn (13), which is used for modelling purely statistical macroscopic cumulative stability constants in coordination chemistry.

$$\beta_{1i}^{\mathrm{M,L}} = C_i^n (k^{\mathrm{M,L}})^i \tag{13}$$

The successive constants $K_i^{\mathrm{M,L}}$ are obtained from eqn (14), and the ultimate ratio $K_{i+1}^{\mathrm{M,L}}/K_i^{\mathrm{M,L}}$ with eqn (15). The latter ratio has been used for decades in coordination chemistry for detecting deviations from statistical binding.[19,21,24]

$$K_i^{\mathrm{M,L}} = \beta_{1i}^{\mathrm{M,L}}/\beta_{1(i-1)}^{\mathrm{M,L}} = \left(C_i^n/C_{i-1}^n\right)k^{\mathrm{M,L}} = \frac{n-i+1}{i}k^{\mathrm{M,L}} \tag{14}$$

$$K_{i+1}^{\mathrm{M,L}}/K_i^{\mathrm{M,L}} = \frac{[(n-i)/(i+1)]k^{\mathrm{M,L}}}{[(n-i+1)/i]k^{\mathrm{M,L}}} = \frac{i(n-i)}{(i+1)(n-i+1)} \tag{15}$$

When eqn (15) is satisfied, the binding is non-cooperative or statistical. If the fixation of one ligand favours the connection of the next one, $K_{i+1}^{\mathrm{M,L}}/K_i^{\mathrm{M,L}}$ is larger than the value predicted by eqn (15), and the process is termed positively cooperative (attractive ligand interactions). The reverse situation, for which the fixation of one ligand hinders the connection of the next one results in $K_{i+1}^{\mathrm{M,L}}/K_i^{\mathrm{M,L}}$ lower than the value predicted by eqn (15), and a negatively cooperative process occurs (repulsive ligand interactions). The latter case is well known for the formation of standard octahedral complexes, for instance the successive binding of ammonia to bivalent nickel in water (equilibrium (16)).[25]

$$\mathrm{Ni^{2+}} + i\,\mathrm{NH_3} \rightleftharpoons [\mathrm{Ni(NH_3)}_i]^{2+}\text{: } \beta_{1i}^{\mathrm{Ni,NH3}} \tag{16}$$

As commonly used in the description of metallosupramolecular self-assembly processes, the solvent molecules are not explicitly considered in equilibrium (16), but it is obvious in this case that each bound ammonia replaces one water molecule around the metal as highlighted in equilibrium (17).

$$[\mathrm{Ni(H_2O)_6}]^{2+} + i\,\mathrm{NH_3} \rightleftharpoons [\mathrm{Ni(H_2O)}_{6-i}\mathrm{(NH_3)}_i]^{2+} + i\,\mathrm{H_2O}\text{: } \beta_{1i}^{\mathrm{Ni,NH3}} \tag{17}$$

The experimental macroscopic stability constants $\beta_{1i}^{\mathrm{Ni,NH3}}$ collected in Table 1,[25] allows the calculation of the successive constants $K_i^{\mathrm{Ni,NH3}}$, together with the ratios $K_{i+1}^{\mathrm{M,L}}/K_i^{\mathrm{M,L}}$, which are systematically lower than the one expected from statistics (eqn (15), Table 1). This feature points to a negatively cooperative

Table 1 Experimental cumulative $\beta_{1i}^{\mathrm{Ni,NH3}}$ and successive $K_i^{\mathrm{Ni,NH3}}$ stability constants for the formation of $[\mathrm{Ni(NH_3)}_i]^{2+}$ (n = 1–6, water, 298 K, equilibrium (16))

Species	$\log(\beta_{1i}^{\mathrm{Ni,NH3}})$	$\log(K_i^{\mathrm{Ni,NH3}})$	$K_{i+1}^{\mathrm{M,L}}/K_i^{\mathrm{M,L}}$	Statistics[a]
$[\mathrm{Ni(NH_3)}]^{2+}$	2.79	2.79	—	—
$[\mathrm{Ni(NH_3)_2}]^{2+}$	5.05	2.26	0.30	0.42
$[\mathrm{Ni(NH_3)_3}]^{2+}$	6.74	1.69	0.27	0.53
$[\mathrm{Ni(NH_3)_4}]^{2+}$	7.99	1.25	0.36	0.56
$[\mathrm{Ni(NH_3)_5}]^{2+}$	8.73	0.74	0.31	0.53
$[\mathrm{Ni(NH_3)_6}]^{2+}$	8.76	0.03	0.19	0.42

[a] Computed with eqn (15).

complexation process, in which the fixation of each successive ammonia hinders the connection to the next one.

Several equivalent graphical tests, which are based on the calculation of the occupancy r, referring to the average number of metallic sites occupied by the ligand (eqn (18)), have been developed in order to assess cooperativity.

$$r = \frac{[\mathrm{L}]_{\mathrm{bound}}}{[\mathrm{M}]_{\mathrm{tot}}} = \frac{[\mathrm{L}]_{\mathrm{tot}} - [\mathrm{L}]}{[\mathrm{M}]_{\mathrm{tot}}} = \frac{\sum_{i=1}^{n} i\,[\mathrm{ML}_i]}{[\mathrm{M}] + \sum_{i=1}^{n} [\mathrm{ML}_i]}$$

$$= \frac{\sum_{i=1}^{n} i\beta_{1i}^{\mathrm{M,L}}\,[\mathrm{M}]\,[\mathrm{L}]^i}{[\mathrm{M}] + \sum_{i=1}^{n} \beta_{1i}^{\mathrm{M,L}}\,[\mathrm{M}]\,[\mathrm{L}]^i} = \frac{\sum_{i=1}^{n} i\beta_{1i}^{\mathrm{M,L}}\,[\mathrm{L}]^i}{1 + \sum_{i=1}^{n} \beta_{1i}^{\mathrm{M,L}}\,[\mathrm{L}]^i} \qquad (18)$$

Since eqn (18) strictly considers the successive intermolecular connection of n ligands to a single receptor (*i.e.* the metal), the final expression for the occupancy r does not depend on its concentration. Introducing eqn (13) into eqn (18) leads to the left hand part of eqn (19), which then can be transformed into polynomials (central part of eqn (19)),[26] and eventually gives the simple Langmuir binding isotherm shown on the right hand part of eqn (19).

$$r = \frac{\sum_{i=1}^{n} i\mathrm{C}_i^n\,(k^{\mathrm{M,L}})^i\,[\mathrm{L}]^i}{1 + \sum_{i=1}^{n} \mathrm{C}_i^n\,(k^{\mathrm{M,L}})^i\,[\mathrm{L}]^i}$$

$$= \frac{nk^{\mathrm{M,L}}\,[\mathrm{L}]\,(1 + k^{\mathrm{M,L}}\,[\mathrm{L}])^{n-1}}{(1 + k^{\mathrm{M,L}}\,[\mathrm{L}])^n} = \frac{nk^{\mathrm{M,L}}\,[\mathrm{L}]}{1 + k^{\mathrm{M,L}}\,[\mathrm{L}]} \qquad (19)$$

Two famous linear forms of eqn (19), known as the Hill plot (eqn (20))[17] and the Scatchard plot (eqn (21))[18] respectively, have been extensively used in biology for testing cooperativity,[16] but they are only rarely found in coordination chemistry.

$$\ln\left(\frac{r}{n-r}\right) = \ln([\mathrm{L}]) + \ln(k^{\mathrm{M,L}}) \qquad (20)$$

$$\frac{r}{[\mathrm{L}]} = -k^{\mathrm{M,L}}\,[\mathrm{L}] + nk^{\mathrm{M,L}} \qquad (21)$$

Since the binding isotherm (eqn (19)) is obtained by using a statistical modelling of the cumulative stability constants (eqn (13)), any deviation from this equation can be assigned to non-cooperative behaviours. Qualitatively, eqn (20) and (21) are well-suited for highlighting such deviations graphically. The Hill plot (eqn (20)) predicts that a plot of $\ln(r/n - r)$ *vs* $\ln([\mathrm{L}])$ is a straight line with a unit slope for statistical binding. Deviations from this behaviour manifest themselves by a S-shaped curve connecting two lines with unit slope (Fig. 7(a)). The value of the slope in the central domain of the curve, known as the Hill coefficient (n_{H}), is a diagnostic criterion for positive ($n_{\mathrm{H}} > 1$) or negative ($n_{\mathrm{H}} < 1$) cooperativity. The construction of the Hill plot for the formation of $[\mathrm{Ni(NH_3)}_i]^{2+}$ (equilibrium (16)) gives $n_{\mathrm{H}} = 0.59$, in line with negative cooperativity (Fig. 7(a)). The alternative Scatchard plot (eqn (21)) is often more easy to use because plots of $r/[\mathrm{L}]$ *vs*. r deviates from the statistical straight line (slope $= -k^{\mathrm{M,L}}$) by showing either concave downward curves or convex upward curves characterizing positive and negative cooperativity, respectively. Fig. 7(b) shows a typical convex curve characterizing the negative

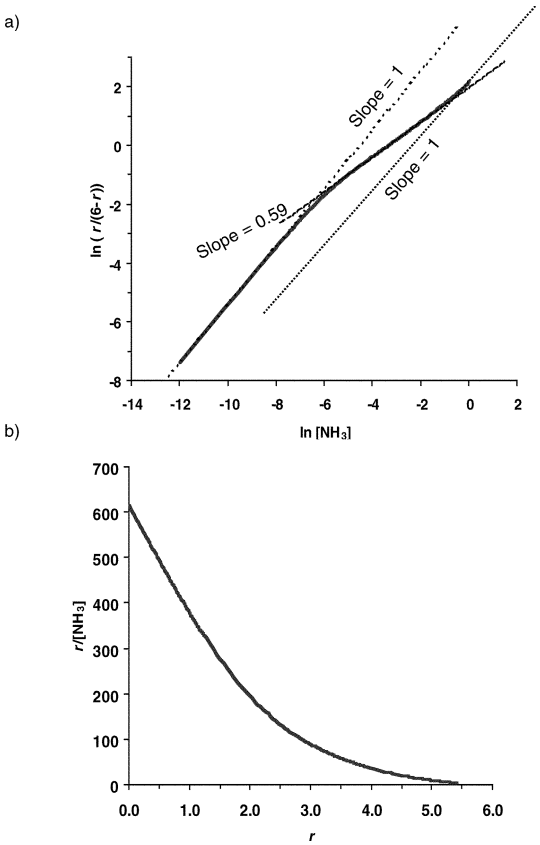

Fig. 7 (a) Hill plot (eqn (20)) and (b) Scatchard plot (eqn (21)) constructed for the successive intermolecular connections of ammonia to bivalent nickel to give $[\mathrm{Ni(NH_3)}_i]^{2+}$ (equilibrium (16), the concentration of the free ligand [L] is computed by using the stability constants collected in Table 1. $[\mathrm{Ni}]^{\mathrm{tot}} = 1 \times 10^{-3}$ M; $[\mathrm{NH_3}]_{\mathrm{tot}}$ varies between 10^{-5} and 1 M).

cooperative processes leading to the formation of $[\mathrm{Ni(NH_3)}_i]^{2+}$ (equilibrium (16)).

Obviously, the consideration of the metal as the receptor to which ligands are successively attached *via* intermolecular connections, can be reversed, and the same model holds for the successive fixation of several metal ions to a single multisite ligand, considered as the receptor (Fig. 8). Statistical binding can be again described with eqn (13) for the macroscopic stability constants $\beta_{i1}^{\mathrm{M,L}}$, except that the total number of n available sites on the metal is replaced by m, which stands for the total number of equivalent sites borne by the ligand, and i corresponds to the fixation of the ith metal. The occupancy r, given in eqn (18), is simply transformed by replacing [L] with [M] (eqn (22)) and the associated binding isotherm (eqn (23)), including the Hill and Scatchard plots, are easily derived by following the same strategy.

$$r = \frac{[\mathrm{M}]_{\mathrm{bound}}}{[\mathrm{L}]_{\mathrm{tot}}} = \frac{[\mathrm{M}]_{\mathrm{tot}} - [\mathrm{M}]}{[\mathrm{L}]_{\mathrm{tot}}} = \frac{\sum_{i=1}^{m} i\,[\mathrm{M}_i\mathrm{L}]}{[\mathrm{L}] + \sum_{i=1}^{m} [\mathrm{M}_i\mathrm{L}]}$$

$$= \frac{\sum_{i=1}^{m} i\beta_{i1}^{\mathrm{M,L}}\,[\mathrm{L}]\,[\mathrm{M}]^i}{[\mathrm{L}] + \sum_{i=1}^{m} \beta_{i1}^{\mathrm{M,L}}\,[\mathrm{L}]\,[\mathrm{M}]^i} = \frac{\sum_{i=1}^{m} i\beta_{i1}^{\mathrm{M,L}}\,[\mathrm{M}]^i}{1 + \sum_{i=1}^{m} \beta_{i1}^{\mathrm{M,L}}\,[\mathrm{M}]^i} \qquad (22)$$

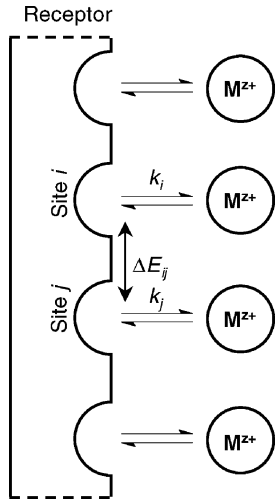

Fig. 8 Thermodynamic protein-ligand model adapted for the successive intermolecular connections of metal ions to an one-dimensional multisite receptor. Reproduced with permission from ref. 23, © Elsevier Science, 2005.

$$r = \frac{mk^{\mathrm{M,L}}[\mathrm{M}]}{1 + k^{\mathrm{M,L}}[\mathrm{M}]} \tag{23}$$

However, this simple model suffers from two main limitations: (1) the use of a unique microscopic affinity $k^{\mathrm{M,L}}$ for each M–L connection (eqn (12) and (13)) restricts the model for the description of receptors possessing m identical binding sites related by C_m or S_m symmetry axes. (2) Deviation from statistical binding is only qualitative. The site binding model accounts for these two specific points thanks to the introduction of (i) a specific microscopic affinity for each binding site $k_i^{\mathrm{M,L}}$ and (ii) a free energy of interaction ΔE_{ij} between the two entering components bound in sites i and j (Fig. 8). The rigorous mathematical treatment of this model by using statistical mechanics has been first proposed for the successive fixation of protons to macromolecules,[27] and then it has been extended for the related connections of metal ions to a single receptor.[28] Let us write the complexation process shown in Fig. 8 with equilibrium (24).

$$m\,\mathrm{M}^{z+} + \mathrm{L} \rightleftharpoons [\mathrm{M}_m\mathrm{L}]^{mz+}\colon \beta_{ml}^{\mathrm{M,L}} \tag{24}$$

Each macrospecies $[\mathrm{M}_m\mathrm{L}]^{mz+}$ is constituted of several microspecies differing in the exact location of the metals bound to the various binding sites of the ligand. Each microspecies can be thus defined by a state vector $\{\boldsymbol{s}_i\}$, for which each element $s_i = 1$ when a metal is bound to site i and $s_i = 0$ when no metal is coordinated. The free energy of complexation $\Delta G(\{\boldsymbol{s}_i\})$ associated with equilibrium (24) for a specific microspecies $[\mathrm{M}_m\mathrm{L}]^{mz+}$ characterized by the state vector $\{\boldsymbol{s}_i\}$ is given in eqn (25), whereby the first term, linear in the state variable s_i, corresponds to the sum of the free energies of intermolecular connection, and the second quadratic term quantitatively estimates the sum of the intermetallic pair interactions (*i.e.*, the interaction between the entering components).

$$\Delta G(\{\boldsymbol{s}_i\}) = -\sum_{i=1}^{m} RT \ln\left(k_i^{\mathrm{M,L}}\right)s_i + \frac{1}{2}\sum_{i=1}^{m}\sum_{j\neq i}^{m}\Delta E_{ij}^{\mathrm{MM}} s_i s_j \tag{25}$$

The cumulative microscopic constant for the formation of the microspecies $[\mathrm{M}_m\mathrm{L}]^{mz+}$ is obtained by using the standard thermodynamic expression $\beta_{ml}^{\mathrm{M,L}}\{\boldsymbol{s}_i\} = \mathrm{e}^{-\Delta G\{s_i\}/RT}$ to give eqn (26), in which we apply the usual notation for the Boltzmann factor $u_{ij}^{\mathrm{MM}} = \mathrm{e}^{-\Delta E_{ij}^{\mathrm{MM}}/RT}$.

$$\begin{aligned}\beta_{m1}^{\mathrm{M,L}}\{\boldsymbol{s}_i\} &= \prod_{i=1}^{m}\left(k_i^{\mathrm{M,L}}\right)^{s_i}\prod_{i<j}^{m}\mathrm{e}^{-(\Delta E_{ij}^{\mathrm{MM}}/RT)^{s_i s_j}} \\ &= \prod_{i=1}^{m}\left(k_i^{\mathrm{M,L}}\right)^{s_i}\prod_{i<j}^{m}\left(u_{ij}^{\mathrm{MM}}\right)^{s_i s_j}\end{aligned} \tag{26}$$

The target macroscopic constant $\beta_{m1}^{\mathrm{M,L}}$ characterizing the formation of the macrospecies $[\mathrm{M}_m\mathrm{L}]^{mz+}$ corresponds to the sum of the different contributing microconstants (eqn (27)).

$$\beta_{m1}^{\mathrm{M,L}} = \sum_{\{\boldsymbol{s}_i\}}\beta_{m1}^{\mathrm{M,L}}\{\boldsymbol{s}_i\} \tag{27}$$

The site binding model (eqns (25)–(27)) can be easily applied for the formation of any polymetallic complex made up of the successive intermolecular fixation of m metal ions to a single ligand (or *vice versa* for the complexation of n ligands to a single metal). For instance, the complexation process described in equilibria (28) and (29) matches the first category because two trivalent europium cations are successively bound to the C_{2v}-symmetrical bis-bidentate ligand $[\mathrm{L11} - 2\mathrm{H}]^{2-}$ (Fig. 9).[29]

$$\begin{aligned}\mathrm{Eu}^{3+} + [\mathrm{L11} - 2\mathrm{H}]^{2-} &\rightleftharpoons [\mathrm{Eu(L11} - 2\mathrm{H})]^{+}\colon K_1^{\mathrm{Eu,L11}} \\ &= \beta_{11}^{\mathrm{Eu,L11}} = 1.9 \times 10^4\end{aligned} \tag{28}$$

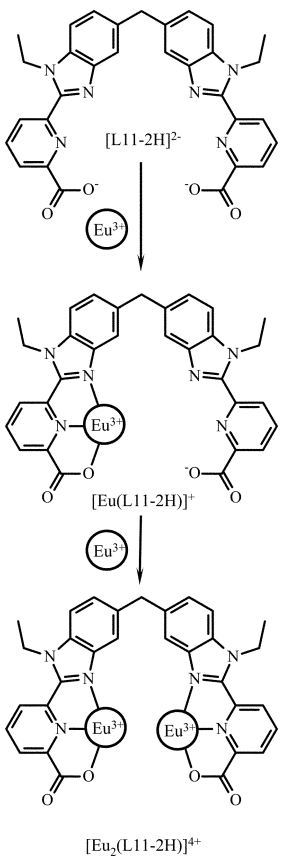

Fig. 9 Schematic formation of the complexes $[\mathrm{Eu(L11} - 2\mathrm{H})]^{+}$ and $[\mathrm{Eu_2(L11} - 2\mathrm{H})]^{4+}$ according to equilibria (28) and (29).

$$2\,Eu^{3+} + [L11 - 2H]^{2-} \rightleftharpoons [Eu_2(L11 - 2H)]^{4+}: \beta_{21}^{Eu,L11} = 2.3 \times 10^6 \quad (29)$$

Since the two binding sites in $[L11 - 2H]^{2-}$ are equivalent, a single microscopic intermolecular affinity $k^{Eu,L11}$ is necessary. Application of eqn (26) gives the microscopic constants $\beta_{11}^{Eu,L11} = k^{Eu,L11}$ (a single Eu–L11 connection and no intermetallic interaction) and $\beta_{21}^{Eu,L11} = (k^{Eu,L11})^2 u^{EuEu}$ (two Eu–L11 connections and one intermetallic interaction $u^{EuEu} = e^{-\Delta E^{EuEu}/RT}$). Transformation into macroconstants with eqn (27) is straightforward since the degeneracy of the microspecies $[Eu(L11 - 2H)]^+$ is $\omega_{11}^{Eu,L11} = 2$ (*i.e.* Eu^{3+} can be bound to any of the two binding sites), while that for $[Eu_2(L11 - 2H)]^{4+}$ is $\omega_{11}^{Eu,L11} = 1$. Eqn (30) and (31) result and their fit with the experimental data of equilibria (28) and (29) gives $\log(k^{Eu,L11}) = 3.98$ and $\Delta E^{EuEu} = 9.1$ kJ mol^{-1}.[23]

$$\beta_{11}^{Eu,L11} = 2k^{Eu,L11} \quad (30)$$

$$\beta_{21}^{Eu,L11} = (k^{Eu,L11})^2 u^{EuEu} \quad (31)$$

The first term refers to the free energy balance between the desolvation of the components (metal and ligand), and their connection in the complexes, while $\Delta E^{EuEu} > 0$ is a direct quantitative estimation of the negative cooperativity accompanying the fixation of Eu^{3+} to $[Eu(L11 - 2H)]^+$. This conclusion can be compared with that arising from the standard coordination approach, which requires the calculation of the ratio of the successive constants $K_2^{Eu,L11}/K_1^{Eu,L11}$ (eqn (15)). From equilibria (28) and (29), the second successive constant is given by

$$Eu^{3+} + [Eu(L11 - 2H)]^+ \rightleftharpoons [Eu_2(L11 - 2H)]^{4+}: K_2^{Eu,L11} = \beta_{21}^{Eu,L11}/\beta_{11}^{Eu,L11} = 1.2 \times 10^2 \quad (32)$$

The experimental ratio $(K_2^{Eu,L11}/K_1^{Eu,L11})_{exp} = 1.2 \times 10^2/1.9 \times 10^4 = 6 \times 10^{-3}$ is smaller than the statistical value calculated with eqn (15) for a total number of $m = 2$ binding sites. The value of $(K_2^{Eu,L11}/K_1^{Eu,L11})_{stat} = 1(2 - 1)/(1 + 1)(2 - 1 + 1) = 0.25$ is in complete agreement with negative cooperativity. However, only the site binding model provides a quantitative estimation of the intermetallic repulsion. Interestingly, the use of the macroconstants modeled in eqn (30) and (31) gives $K_2^{Eu,L11}/K_1^{Eu,L11}$ shown in eqn (33), which demonstrates that any deviation from the statistical value $(K_2^{Eu,L11}/K_1^{Eu,L11})_{stat} = \frac{1}{4}$ is measured by $u^{EuEu} \neq 1$ (*i.e.* $\Delta E^{EuEu} \neq 0$).

$$K_2^{Eu,L11}/K_1^{Eu,L11} = \beta_{21}^{Eu,L11}/(\beta_{11}^{Eu,L11})^2 = u^{EuEu}/4 \quad (33)$$

Moreover, the site binding model has the advantage of being able to address systems possessing non-equivalent binding sites, a situation which escapes the standard treatment proposed in eqn (13)–(15). As an example, let us consider the successive fixation of two Fe^{3+} to the ligand L12 to give [Fe(L12)] and $[Fe_2(L12)]$ (Fig. 10, equilibria (34) and (35)).[30]

$$Fe^{3+} + L12 \rightleftharpoons [Fe(L12)]: \log(\beta_{11}^{Fe,L12}) = 5.82 \quad (34)$$

$$2\,Fe^{3+} + L12 \rightleftharpoons [Fe_2(L12)]: \log(\beta_{21}^{Fe,L12}) = 12.14 \quad (35)$$

[Fe(L12)] may exist as two microspecies, in which Fe^{3+} is bound either to the internal ($k_{int}^{Fe,L12}$) or to the external ($k_{ext}^{Fe,L12}$) cavity. The

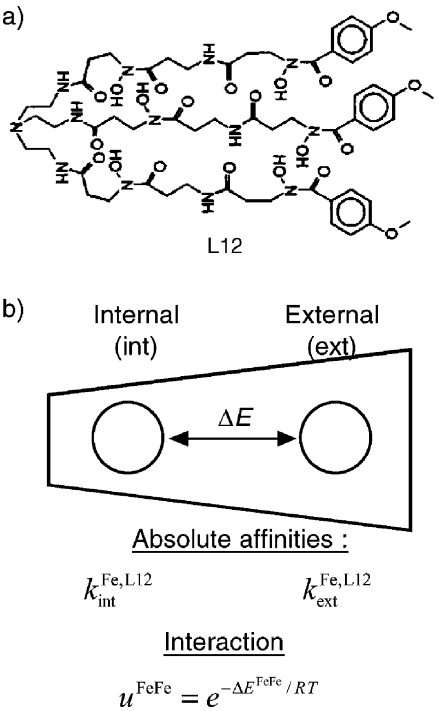

Fig. 10 (a) Chemical structure of the ligand L12 and (b) associated site-binding model with microscopic parameters.

macroscopic constant combines both microscopic constants (eqn (27)) to give

$$\beta_{11}^{Fe,L12} = k_{int}^{Fe,L12} + k_{ext}^{Fe,L12} \quad (36)$$

On the other hand, $[Fe_2(L12)]$ exists as a single microspecies and its macroscopic constant is simply obtained with eqn (26) to give

$$\beta_{21}^{Fe,L12} = (k_{int}^{Fe,L12})(k_{ext}^{Fe,L12})u^{FeFe} \quad (37)$$

Taking the macroconstants in eqn (36) and (37), we can again calculate the ratio of the successive constants $K_2^{Fe,L12}/K_1^{Fe,L12}$ (eqn (38)). In this case, a statistical behaviour (*i.e.* non-cooperative with $u^{FeFe} = 1$) corresponds to a complicated ratio of microscopic constants (eqn (38)).

$$K_2^{Fe,L12}/K_1^{Fe,L12} = \frac{\beta_{21}^{Fe,L12}}{\left(\beta_{11}^{Fe,L12}\right)^2} = \frac{k_{int}^{Fe,L12}k_{ext}^{Fe,L12}}{\left(k_{int}^{Fe,L12} + k_{ext}^{Fe,L12}\right)^2}u^{FeFe} \quad (38)$$

Since the determination of three microscopic parameters $k_{int}^{Fe,L12}$, $k_{ext}^{Fe,L12}$ and u^{FeFe} with only two accessible macroscopic constants (equilibria (34) and (35)) is impossible, *cooperativity cannot be addressed*, except if the two microscopic constants characterizing [Fe(L12)] could be separately estimated. A common approximation considers the two binding sites as equivalent with $k_{int}^{Fe,L12} \cong k_{ext}^{Fe,L12}$, and eqn (38) reduces to $K_2^{Fe,L12}/K_1^{Fe,L12} = u^{FeFe}/4$. This approximation is universally used in biology for the multivalent complexation of ligands to the different sites of a protein, because the latter receptor generally does not possess the C_n (or S_n) symmetry axes required for a strict equivalence of the n binding sites. Based on this approximation, the authors of ref. 30 conclude that their experimental ratio $K_2^{Fe,L12}/K_1^{Fe,L12} = 3.2$, which is larger than $\frac{1}{4}$, is diagnostic for positive cooperativity. It is worth stressing that the use of ratios of successive constants (eqn (15)), Hill plots (eqn (20))

and Scatchard plots (eqn (21)) are only relevant to successive intermolecular complexation processes involving equivalent sites, a situation rarely encountered in practice. The pseudo-equivalence approximation is thus a very common approach, particularly in biology,[16] although it is rarely unambiguously mentioned. According to the complexity of the assembly processes leading to supramolecular polymetallic complexes, which mix intramolecular and intermolecular connections (see for instance equilibria (1)–(7)), standard tests for cooperativity limited to intermolecular complexation processes are of little use. However, an extension of the site binding model for the analysis of more complicated systems has been first proposed for polymetallic lanthanide-containing helicates $[Ln_2(L13)_3]^{6+}$ (Fig. 11) and $[Ln_3(L3)_3]^{9+}$ (Fig. 12), and then applied to the trimetallic sandwich complexes $[Ln_3(L14 - 3H)_2]^{3+}$ (Fig. 13).[23,28,31,32]

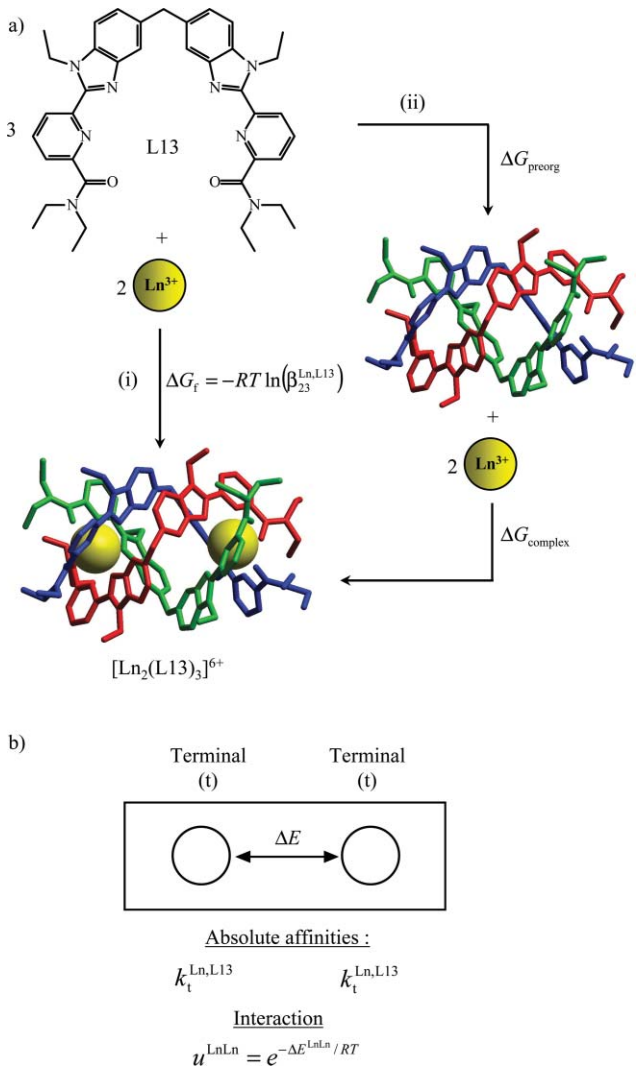

Fig. 11 (a) Formation and solution structures of $[Ln_2(L13)_3]^{6+}$ showing the complete assembly process (ΔG_f, path (i)), and its partition into one virtual preorganization step (ΔG_{preorg}) followed by intermolecular complexations ($\Delta G_{complex}$, path (ii)). (b) Associated thermodynamic site binding model.[31]

We first focus on the simple formation of the bimetallic triple-stranded helicate $[Ln_2(L13)_3]^{6+}$, in which the two coordination sites are equivalent (Fig. 11). Please note that the reaction of three L13 with two Ln^{3+} (equilibrium (39)) does not correspond to strictly intermolecular complexation processes to a single receptor, the criterion required for simply applying the protein-ligand or the site binding model.

$$2\,Ln^{3+} + 3\,L13 \rightleftharpoons [Ln_2(L13)_3]^{6+}: \beta_{23}^{Ln,L13} \quad (39)$$

In order to force equilibrium (39) to match the criterion of the successive fixation of two Ln^{3+} to a single receptor, the free energy of formation of $[Ln_2(L13)_3]^{6+}$, $\Delta G_f = -RT \ln(\beta_{23}^{Ln,L13})$ (equilibrium (39), Fig. 11(a), path (i)), is partitioned into a first process providing the virtual preorganized receptor $(L13)_3$, (ΔG_{preorg} in equilibrium (40), Fig. 11(a), path (ii)) followed by purely intermolecular complexation of Ln^{3+} ($\Delta G_{complex}$ in equilibrium (41), Fig. 11(a), path (ii)).

$$3\,L13 \rightleftharpoons (L13)_3: \Delta G_{preorg} \quad (40)$$

$$2\,Ln^{3+} + (L13)_3 \rightleftharpoons [Ln_2(L13)_3]^{6+}: \Delta G_{complex} \quad (41)$$

We can eventually write

$$\Delta G_f = -RT \ln(\beta_{23}^{Ln,L13}) = \Delta G_{preorg} + \Delta G_{complex} \quad (42)$$

The second complexation term $\Delta G_{complex}$ can be modeled with the site binding model (eqn (25)–(27)) operating on the preorganized receptor $(L13)_3$. ΔG_{preorg} is more difficult to assess, but it similarly affects any complex made up of the same triple-helical box shown in Fig. 11. If we restrict the analysis of the self-assembly of $[Ln_2(L13)_3]^{6+}$ to complexes containing the same organization of the $(L13)_3$ box, ΔG_{preorg} only corresponds to a translation of the zero-level of the free energy of formation, and it can be arbitrarily set to $\Delta G_{preorg} = 0$. In these special conditions, eqn (42) reduces to $\Delta G_{complex} = -RT \ln(\beta_{23}^{Ln,L13})$ and the site binding model (eqn (25)–(27)) can be applied, according that the interpretation of the microscopic affinity explicitely considers both hypotheses: (1) only complexes with similar preorganized receptors are considered and (2) $\Delta G_{preorg} = 0$. Application of eqn (26) and (27) for the formation of the final complex $[Ln_2(L13)_3]^{6+}$ with a single microscopic affinity constant $k_t^{Ln,L13}$ for the terminal N_6O_3 binding site leads to eqn (43) (Fig. 11(b)). Interestingly, NMR data demonstrate that the intermediate complex $[Ln(L13)_3]^{3+}$ (equilibrium (44)) strictly adopts a facial organization of the three strands compatible with its modelling as a $(L13)_3$ box, to which one Ln^{3+} is connected (eqn (45)).[31]

$$\beta_{23}^{Ln,L13} = (k_t^{Ln,L13})^2 u^{LnLn} \quad (43)$$

$$Ln^{3+} + (L13)_3 \rightleftharpoons [Ln(L13)_3]^{3+}: \Delta G_{complex} \quad (44)$$

$$\beta_{13}^{Ln,L13} = 2(k_t^{Ln,L13}) \quad (45)$$

The simultaneous consideration of eqn (43) and (45) for the two experimental macroscopic constants $\beta_{13}^{Ln,L13}$ and $\beta_{23}^{Ln,L13}$ determined for each lanthanide,[31] allows the calculation of the two microscopic parameters $\log(k_t^{Ln,L13})$ and ΔE^{LnLn} shown in Fig. 14.

Since the zero-level of the free energy has been arbitrarily fixed to $\Delta G_{preorg} = 0$, the microscopic free energy $\Delta g_t^{Ln,L13} = -RT \ln(k_t^{Ln,L13})$ has no direct physical interpretation. However the comparison between the various $\Delta g_t^{Ln,L13}$ obtained for different lanthanides makes sense and the plots of Fig. 14(a) points to a weak preference of $(L13)_3$ for mid-range Ln^{3+}. The contribution

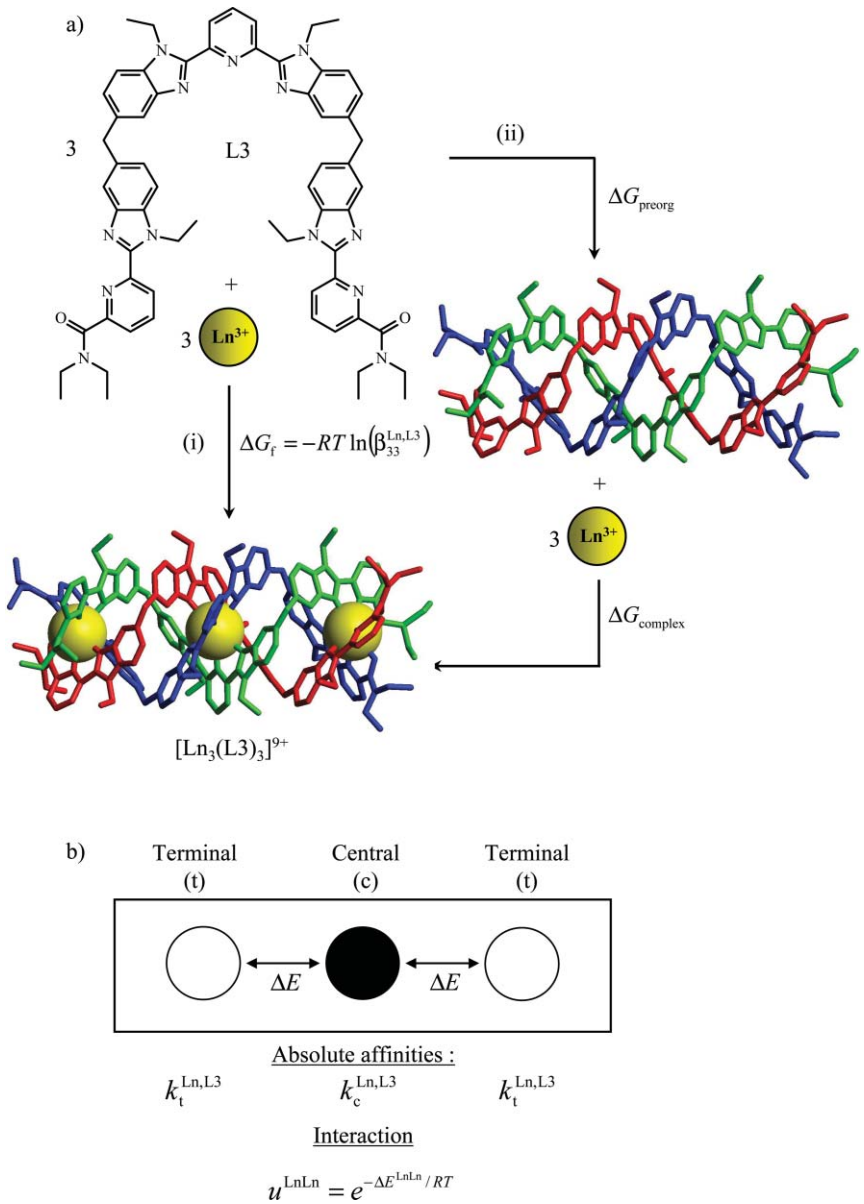

Fig. 12 (a) Formation and solution structures of $[Ln_3(L3)_3]^{9+}$ showing the complete assembly process (ΔG_f, path (i)), and its partition into one virtual preorganization step (ΔG_{preorg}) followed by intermolecular complexations ($\Delta G_{complex}$, path (ii)). (b) Associated thermodynamic site binding model.[31]

ΔE^{LnLn} measures the extra energy cost associated with the intermetallic interaction resulting from the connection of two adjacent metals. We observe that $\Delta E^{LnLn} > 0$ for all lanthanides (Fig. 14(b)), which unambiguously demonstrates negative cooperativity for the successive fixation of the two metal ions. Moreover, ΔE^{LnLn} does not deviate significantly from its average value $\Delta E^{LnLn} = 51(7)$ kJ mol^{-1}, which is well comparable to $\Delta E^{LnLn} = 48$ kJ mol^{-1} computed for the electrostatic work required for approaching two triply charged Ln^{3+} cations at 9.06 Å in acetonitrile (*i.e.* the solvent in which the self-assembly of $[Ln_2(L13)_3]^{6+}$ has been investigated).[31]

The same approach has been used for modelling the formation of (i) the trimetallic triple-stranded helicates $[Ln_3(L3)_3]^{9+}$ (equilibria (5)–(7) and Fig. 12(a)), in which the central N_9 binding site k_c^{LnL3} is different from the terminal N_6O_3 sites $k_t^{Ln,L13}$ (Fig. 12(b))[31] and (ii) the trimetallic sandwich complexes $[Ln_3(L14 - 3H)_2]^{3+}$ (equilibrium (46) and Fig. 13).[23,28,32] In both cases, negative cooperativity ($\Delta E^{LnLn} > 0$) operates.

$$3\,Ln^{3+} + 2\,[L14 - 3H]^{3-} \rightleftharpoons [Ln_3(L14 - 3H)_2]^{3+}: \beta_{32}^{Ln,L14} \qquad (46)$$

A questionable simultaneous treatment of the bimetallic $[Ln_2(L13)_3]^{6+}$ and trimetallic $[Ln_3(L3)_3]^{9+}$ helicates has been attempted in order to increase the number of accessible macroscopic constants for fitting a common set of three microscopic parameters k_t^{Ln}, k_t^{Ln} and ΔE^{LnLn}.[31b] However, this approach is only valid if ΔG_{preorg} is similar for the virtual formation of $(L13)_3$ (Fig. 11(a)) and $(L3)_3$ (Fig. 12(a)), an assumption which has still not been unambiguously demonstrated. Although the introduction of the concept of virtually preorganized receptors fixing the zero-level of the free energy allows the use of the simple site binding model for addressing intermetallic interaction, hence cooperativity, it

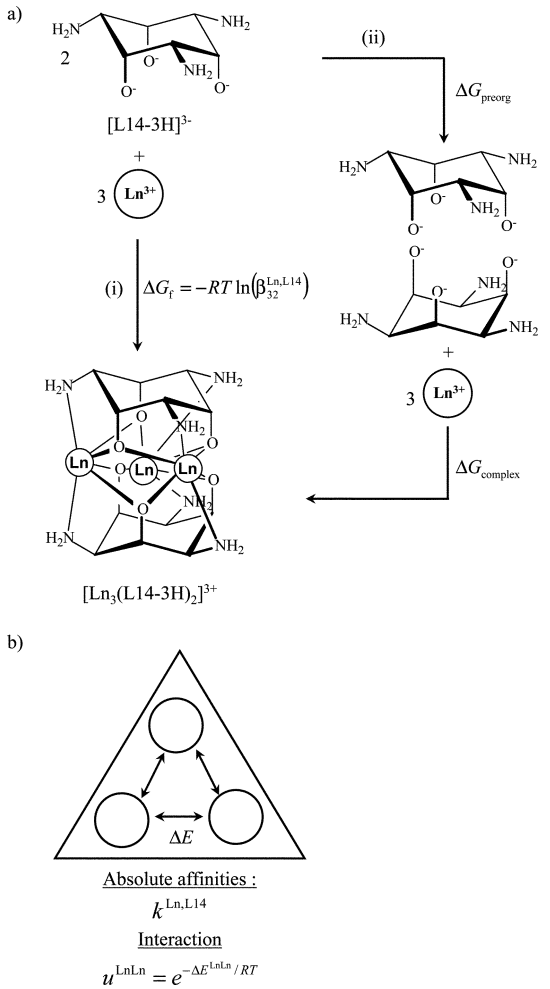

Fig. 13 (a) Formation and solution structures of $[Ln_3(L14 - 3H)_2]^{3+}$ showing the complete assembly process (ΔG_f, path (i)), and its partition into one virtual preorganization step (ΔG_{preorg}) followed by intermolecular complexations ($\Delta G_{complex}$, path (ii)). (b) Associated thermodynamic site binding model.[23,28]

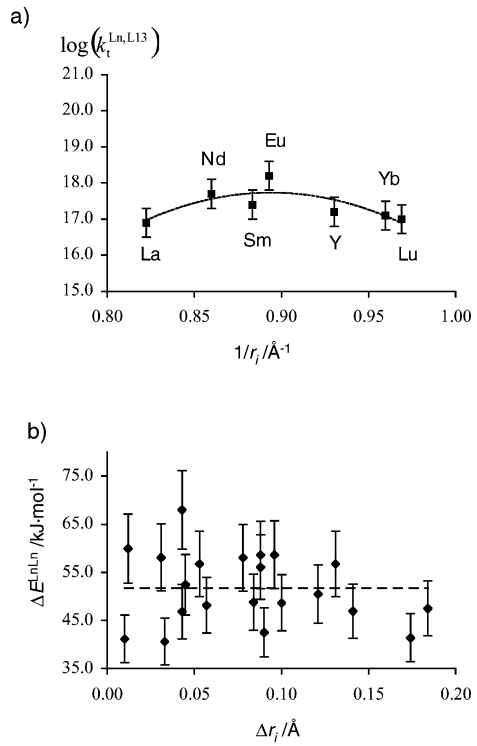

Fig. 14 (a) Computed absolute affinities for the terminal sites ($\log(k_t^{Ln,L13})$) and (b) intermetallic interaction parameters (ΔE^{LnLn}) in the triple-stranded bimetallic helicates $[Ln_2(L13)_3]^{6+}$ as a function of the inverse of nine-coordinate ionic radii of the lanthanides ($\Delta r_i = |r_{Ln^1} - r_{Ln^2}|$). Adapted from ref. 31*b*.

remains strictly limited to a series of complexes possessing the same arrangement of the ligands in the receptor.

3 Modeling multicomponent complexation processes involving intra- and intermolecular connections: Ercolani's model

The unravelling of the competition between intra- and intermolecular connection processes has a long history in polymer chemistry, because of the need for finding conditions in which polymerization (*i.e.* intermolecular connection, path (a) in Fig. 15) is preferred over cyclization (*i.e.* intramolecular connection, path (b) in Fig. 15).[33]

An empirical experimental parameter EM, termed the effective molarity (because of its formal concentration units) has been extensively used as a measure of the ease of intramolecular connection with respect to the alternative intermolecular process (Fig. 15 and eqn (47)).[33c] Expressed as free energies in eqn (48), we realize that $-RT\ln(EM)$ indeed corresponds to the correction

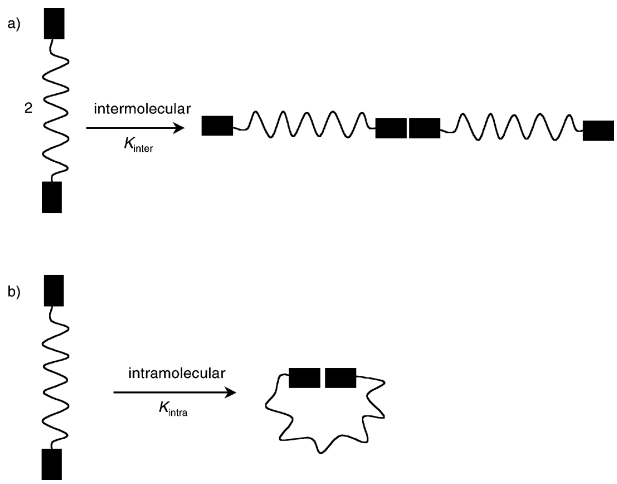

Fig. 15 Competition between (a) intermolecular and (b) intramolecular connection processes.

which applies when the intermolecular process is replaced by the intramolecular one.[33]

$$EM = K_{intra}/K_{inter} \quad (47)$$

$$-RT\ln(EM) = -RT\ln(K_{intra}) + RT\ln(K_{inter}) = \Delta G_{intra} - \Delta G_{inter} \quad (48)$$

If we now introduce the enthalpic and entropic contributions to each type of connection, eqn (48) transforms into eqn (49), which

further reduces to a pure entropic correction when a strainless ring is formed (*i.e.* $\Delta H_{intra} \approx \Delta H_{inter}$).

$$-RT\ln(EM) = (\Delta H_{intra} - \Delta H_{inter}) - T(\Delta S_{intra} - \Delta S_{inter}) \approx -T(\Delta S_{intra} - \Delta S_{inter}) \quad (49)$$

The experimental effective molarity *EM* is often replaced by the identical, but theoretical concept of effective concentration c^{eff},[33cj] and we will use this terminology for the rest of our discussion. With this novel terminology, eqn (49) transforms into eqn (50), and its introduction into eqn (47) shows that c^{eff} is a pure entropic correction, which applies when an intermolecular process is replaced by its intramolecular counterpart (eqn (51)).

$$c^{eff} = e^{(\Delta S_{intra} - \Delta S_{inter})/R} \quad (50)$$

$$K_{intra} = c^{eff} K_{inter} = e^{(\Delta S_{intra} - \Delta S_{inter})/R} K_{inter} \quad (51)$$

The same approach holds for microscopic connection processes, and Ercolani proposed that the microscopic cumulative constant $\beta_{mn}^{M,L}$ of any multicomponent self-assembly process described by equilibrium (52) can be obtained in absence of intermetallic and interligand interactions, by combining intra- and intermolecular processes in eqn (53), as previously done for purely intermolecular processes in eqn (13) ($\omega_{mn}^{M,L}$ is the degeneracy of the microspecies $[M_mL_n]$).[21]

$$m\,M + n\,L \rightleftharpoons [M_mL_n]: \beta_{mn}^{M,L} \quad (52)$$

$$\beta_{mn}^{M,L} = \omega_{mn}^{M,L} \prod_{intra} k_{intra}^{M,L} \prod_{inter} k_{inter}^{M,L} \quad (53)$$

Let us illustrate the use of eqn (53) for the formation of the complex $[M_2L_2]$ shown in Fig. 16. The three first steps strictly correspond to intermolecular metal–ligand connections, each represented by the microscopic affinity $k_{inter}^{M,L}$. The fourth step refers to an intramolecular cyclization characterized by $k_{intra}^{M,L}$. Ercolani was the first to use eqn (53) for dissecting multicomponent metal–ligand complexation processes involving intra- and intermolecular processes.[21] According to the principle of maximum site occupancy, the assembly of ligands possessing *m* binding sites with metal having *n* coordination sites provides a complex $[M_mL_n]$ (equilibrium (52)), in which the $N = m + n$ components are linked by $B = mn$ connections, among which $N - 1$ are intermolecular and $B - (N - 1) = B - N + 1 = mn - m - n + 1$ are intramolecular.[21] Eqn (53) thus transforms into eqn (54), in which $\sigma_{mn}^{M,L}$ is a symmetry factor characterizing the change in degeneracy of the microspecies involved in the assembly process (including the formation of enantiomers when necessary).[21]

$$\beta_{mn}^{M,L} = \sigma_{mn}^{M,L} (k_{intra}^{M,L})^{mn-m-n+1} (k_{inter}^{M,L})^{m+n-1} \quad (54)$$

We notice that eqn (54) is strictly similar to eqn (13), except that the latter is restricted to intermolecular connection processes, while Ercolani's model (eqn (54)) also holds for more sophisticated complexation reactions involving intra and intermolecular processes. Assuming that $k_{inter}^{M,L}$ and $k_{intra}^{M,L}$ have been estimated from the consideration of two experimental macroscopic constants within a self-assembly process, the stability of any related complex $[M_mL_n]$ can be predicted with eqn (54). Cooperativity, non-cooperativity and negative cooperativity is evidenced when the experimental macroscopic constant $\beta_{mn}^{M,L}$ is respectively larger, equal and lower than that predicted with eqn (54). The assembly of Lehn's double-stranded helicates (equilibria (1)–(4)) has been analyzed by Ercolani as an illustration of the potential of his model.[21] The consideration of equilibrium (2), which strictly refers to two successive intermolecular Cu–L2 connections allowed the unambiguous estimation of $k_{inter}^{Cu,L2}$ as the only adjustable parameter in eqn (54). The subsequent modelling of equilibrium (3), which involves both intra- and intermolecular processes, with eqn (54) provides $k_{intra}^{Cu,L2}$ by using the previously estimated value of $k_{inter}^{Cu,L2}$.[21] With these microscopic parameters at hands, Ercolani predicted $\beta_{32}^{Cu,L2} = 18.25$ for equilibrium (3), a value which compares favourably with the experimental data 18.6.[21] Ercolani thus concluded that the formation of the double-stranded helicate $[Cu_3(L2)_2]^{3+}$ corresponds to a non-cooperative process,[21] an assumption which sounds as a strong argument against the original claim for positive cooperativity[15] based on the use of the protein-ligand model for unravelling multicomponent self-assemblies leading to metallosupramolecular complexes. However, this attractive simple

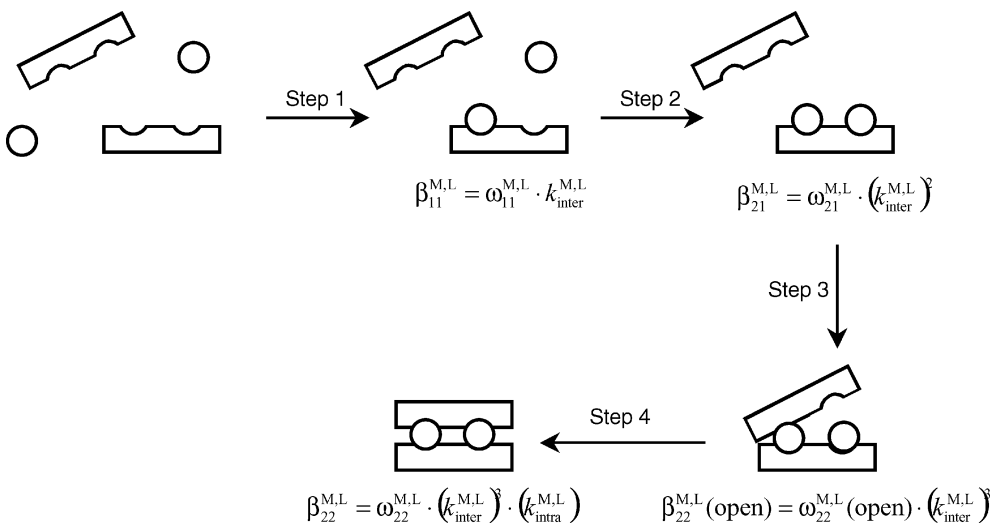

Fig. 16 Schematic formation of the complex $[M_2L_2]$ and its modelling with Ercolani's model (eqn (54)).

model, summarized in eqn (54), suffers from two limitations: (1) since a single pair of microscopic affinities is considered ($k_{\text{intra}}^{\text{M,L}}$ and $k_{\text{inter}}^{\text{M,L}}$), only assemblies involving strictly equivalent (or at least pseudo-equivalent) binding sites can be analyzed (this is indeed the same limitation already encountered for the protein-ligand model for strictly intermolecular connections). (2) The origin of the deviations from statistical binding, *i.e.* cooperativity, is not clearly assigned to extra energy costs arising from intercomponents interactions, which are not considered in the metal–ligand connections taken as the basis for the statistical description of the assembly. In other words, the intermetallic (ΔE^{MM}) and interligand (ΔE^{LL}) interactions are partitioned within $k_{\text{inter}}^{\text{M,L}}$ and $k_{\text{intra}}^{\text{M,L}}$ during the parametrization steps (eqn (54)), and their magnitudes depend on the equilibria, which have been selected as references. For instance, equilibria (2) and (3) have been used for extracting $k_{\text{inter}}^{\text{Cu,L2}}$ and $k_{\text{intra}}^{\text{Cu,L2}}$ in the self-assembly of $[Cu_3(L2)_2]^{3+}$.[21] If the free energy contribution arising from the intermetallic and interligand interactions is roughly proportional to the total number of metal–ligand connections within a series of homologous complexes, as it is the case for the assemblies of the helicates $[Cu_3(L2)_2]^{3+}$,[34] and $[Ln_3(L3)_3]^{3+}$,[31,34] then Ercolani's model indeed tests whether $k_{\text{inter}}^{\text{M,L}}$ and $k_{\text{intra}}^{\text{M,L}}$, originally obtained for the two reference complexes, also hold for the prediction of the next higher homologue. Consequently, this model detects whether $k_{\text{inter}}^{\text{M,L}}$ and $k_{\text{intra}}^{\text{M,L}}$ vary along a series of closely related complexes, whatever the sign of ΔE^{LL} and ΔE^{MM}. To our opinion, such a test better refers to *repetitive statistical binding* along a series of homologous polymetallic complexes,[23,31b] and we limit the terms of cooperative (negatively or positively) and non-cooperative processes to the interpretation of the sign of the total extra energy change arising from intermetallic and interligand interactions (*vide supra* in eqn (59)).

4 Addressing cooperativity in multicomponent complexation processes involving intra- and intermolecular connections: the extended site binding model

As previously done for adapting the protein-ligand model (eqn (13)) for the explicit consideration of the intermetallic interactions (or the interligand interactions) as the origin of cooperativity in strictly intermolecular complexation processes (eqn (26)), Ercolani's model (eqn (54)) can be adapted for assigning the origin of deviation from statistical behaviours (*i.e.* cooperativity) to the combination of intermetallic and interligand interactions. In 2005, Hamacek *et al.* proposed a complete analysis of the free energy of formation of complicated microscopic polymetallic complexes $[M_mL_n]$ (equilibria (52)) with the explicit consideration of five different contributions (eqn (55)).[35]

$$\Delta G_{mn}^{\text{M,L}} = -RT\ln\left(\beta_{mn}^{\text{M,L}}\right) = -RT\ln\left(\sigma_{\text{chir}}^{\text{M,L}}\omega_{mn}^{\text{M,L}}\right) - \sum_{i=1}^{m\cdot n} RT\ln\left(k_i^{\text{M,L}}\right) - \sum_{i=1}^{m\cdot n-m-n+1} RT\ln\left(c_i^{\text{eff}}\right) + \sum_{i<j}{}'' \left(\Delta E_{ij}^{\text{MM}}\right) + \sum_{k<l}{}''' \left(\Delta E_{kl}^{\text{LL}}\right) \quad (55)$$

(1) $-RT\ln(\sigma_{\text{chir}}^{\text{M,L}}\omega_{mn}^{\text{M,L}})$ represents the contribution of the degeneracy of the microscopic state, whereby $\sigma_{\text{chir}}^{\text{M,L}}$ accounts for the entropy of mixing of enantiomers ($\sigma_{\text{chir}}^{\text{M,L}} = 2$ when chirality is created during the complexation process and $\sigma_{\text{chir}}^{\text{M,L}} = 1$ in other cases). $\omega_{mn}^{\text{M,L}}$ is the number of equivalent microspecies, which contribute to the microscopic state.

(2) $-\sum_{i=1}^{mn} RT\ln\left(k_i^{\text{M,L}}\right)$ corresponds to the sum of the microscopic free energies of metal–ligand connections, when all are considered as arising from strictly intermolecular processes. The total number of connections *mn* assumes that the principle of maximum site occupancy is obeyed.[21]

(3) $-\sum_{i=1}^{mn-m-n+1} RT\ln\left(c_i^{\text{eff}}\right)$ represents the sum of all entropic corrections (eqn (50)) affecting the $mn - m - n + 1$ intramolecular connections existing in the $[M_mL_n]$ complex. Combining terms 2 and 3 leads to eqn (56). The introduction of eqn (51) easily demonstrates that terms 2 and 3 indeed corresponds to Ercolani's model (eqn (54)) in its logarithmic form.

$$\begin{aligned} &-\sum_{i=1}^{mn} RT\ln\left(k_i^{\text{M,L}}\right) - \sum_{i=1}^{mn-m-n+1} RT\ln\left(c_i^{\text{eff}}\right) \\ &= -\sum_{i=1}^{m+n-1} RT\ln\left(k_i^{\text{M,L}}\right) - \sum_{i=1}^{mn-m-n+1} RT\ln\left(c^{\text{eff}}k_i^{\text{M,L}}\right) \\ &= -RT\left\{\sum_{i=1}^{m+n-1}\ln\left(k_{\text{inter}}^{\text{M,L}}\right) + \sum_{i=1}^{mn-m-n+1}\ln\left(k_{\text{intra}}^{\text{M,L}}\right)\right\} \end{aligned} \quad (56)$$

(4) $\sum_{i<j}{}''\left(\Delta E_{ij}^{\text{MM}}\right)$ corresponds to the sum of all intermetallic interactions occurring in the final $[M_mL_n]$ complex. This sum can be limited to short-range interactions affecting occupied adjacent sites, but it can be also extended to include long-range interactions. According to a simple electrostatic model assuming a constant local dielectric constant for the medium separating the metals, we expect $\Delta E_{ij}^{\text{MM}} \propto r_{ij}^{-1}$, whereby r_{ij} is the separation between the metals occupying the sites *i* and *j*.

(5) $\sum_{k<l}{}'''\left(\Delta E_{kl}^{\text{LL}}\right)$ refers to the sum of the interligand interactions occurring in the final $[M_mL_n]$ complex. These interactions operate when two ligands bound to the same metal, in agreement with a similar definition used in the site binding model, when ligands are successively attached to the same metal ion. This is illustrated for the formation $[Ni(NH_3)_i]^{2+}$, which is modeled with $\beta_{1i}^{\text{Ni,NH3}} = C_i^6(k^{\text{Ni,NH3}})^i(u^{\text{LL}})^{i(i-1)/2}$ because the fixation of *i* ammonia to a pseudo-octahedral Ni^{2+} cation produces $i(i-1)/2$ metal-mediated interligand interactions.[35] Again, refined interaction modes can be easily implemented depending on the exact system under investigation.

Straightforward algebra transforms eqn (55) into eqn (57), which appears suitable for correlating experimentally accessible microscopic constants with the various parameters.

$$\beta_{mn}^{M,L} = \left(\sigma_{\text{chir}}^{\text{M,L}}\omega_{mn}^{\text{M,L}}\right)\prod_{i=1}^{mn}\left(k_i^{\text{M,L}}\right)\prod_{i=1}^{mn-m-n+1}\left(c_i^{\text{eff}}\right) \times \prod_{i<j}{}''\left(e^{-\frac{\Delta E_{ij}^{\text{MM}}}{RT}}\right)\prod_{k<l}{}'''\left(e^{-\frac{\Delta E_{kl}^{\text{LL}}}{RT}}\right) \quad (57)$$

The introduction of the usual terminology for the interaction parameters as Boltzmann's factors $u_{ij}^{\text{MM}} = e^{-\frac{\Delta E_{ij}^{\text{MM}}}{RT}}$ and $u_{kl}^{\text{LL}} = e^{-\frac{\Delta E_{kl}^{\text{LL}}}{RT}}$

leads to the final compact formulation given in eqn (58).[35]

$$\beta_{mn}^{M,L} = \left(\sigma_{chir}^{M,L}\omega_{mn}^{M,L}\right)\prod_{i=1}^{mn}\left(k_i^{M,L}\right)\prod_{i=1}^{mn-m-n+1}\left(c_i^{eff}\right) \times \prod_{i<j}{}''\left(u_{ij}^{MM}\right)\prod_{k<l}{}'''\left(u_{kl}^{LL}\right) \quad (58)$$

It is worth noting that for purely successive intermolecular connections of metals to a single ligand, as found for the formation of $[Eu_2(L11 - 2H)]^{4+}$ (equilibria (28) and (29)), $c_i^{eff} = 1$ and $u_{kl}^{LL} = 1$ (*i.e.* $\Delta E_{ij}^{LL} = 0$), and eqn (58) (extended site binding model) reduces to eqn (26) (site binding model). Let us apply eqn (58) for modelling the formation of the complex $[M_2L_2]$ (Fig. 17), a process previously analyzed by using Ercolani's model in Fig. 16.

Comparing Fig. 16 and 17 shows that the extended site binding model (Fig. 17) is related to Ercolani's approach (Fig. 16), except for the explicit description of the extra energy cost associated with interactions between the entering components (ΔE^{MM} and ΔE^{LL}). Since cooperativity, assigned to deviation from statistical binding, depends on these two terms, their sum in the global free energy term ΔE_{dev} can be used as a reliable criterion for a quantitative estimation of this deviation in multicomponent self-assembly processes (eqn (59)). For an assembly involving two different components, metals and ligands, in eqn (58), $\Delta E_{dev} > 0$, $\Delta E_{dev} = 0$ and $\Delta E_{dev} < 0$ correspond to negatively cooperative, non-cooperative and positively cooperative processes, respectively.

$$\Delta E_{dev} = \sum_{i<j}{}''\left(\Delta E_{ij}^{MM}\right) + \sum_{k<l}{}'''\left(\Delta E_{kl}^{LL}\right) \quad (59)$$

The formation of the bimetallic triple-stranded helicate $[Eu_2(L11 - 2H)_3]$ is well suited for illustrating the use of eqn (58) for dissecting the different contributions, because detailed kinetic[29] and thermodynamic[36] studies provide five accessible macroscopic constants (equilibria (28′), (29′), (60)–(62), $\log(\beta_{mn}^{Eu,L11})$ are given as conditional stability constants at pH = 6.15 in water, Fig. 18).[23]

$$Eu^{3+} + [L11 - 2H]^{2-} \rightleftharpoons [Eu(L11 - 2H)]^{+}: \log(\beta_{11}^{Eu,L11}) = 4.4 \quad (28')$$

$$2\,Eu^{3+} + [L11 - 2H]^{2-} \rightleftharpoons [Eu_2(L11 - 2H)]^{4+}: \log(\beta_{21}^{Eu,L11}) = 6.4 \quad (29')$$

$$Eu^{3+} + 2\,[L11 - 2H]^{2-} \rightleftharpoons [Eu(L11 - 2H)_2]^{-}: \log(\beta_{12}^{Eu,L11}) = 9.3 \quad (60)$$

$$2\,Eu^{3+} + 2\,[L11 - 2H]^{2-} \rightleftharpoons [Eu_2(L11 - 2H)_2]^{2+}: \log(\beta_{22}^{Eu,L11}) = 16.0 \quad (61)$$

$$2\,Eu^{3+} + 3\,[L11 - 2H]^{2-} \rightleftharpoons [Eu_2(L11 - 2H)_3]: \log(\beta_{23}^{Eu,L11}) = 26.1 \quad (62)$$

Since the two binding sites are equivalent in the C_{2v}-symmetrical ligand $[L11 - 2H]^{2-}$, a single microscopic affinity $k^{Eu,L11}$ is required,

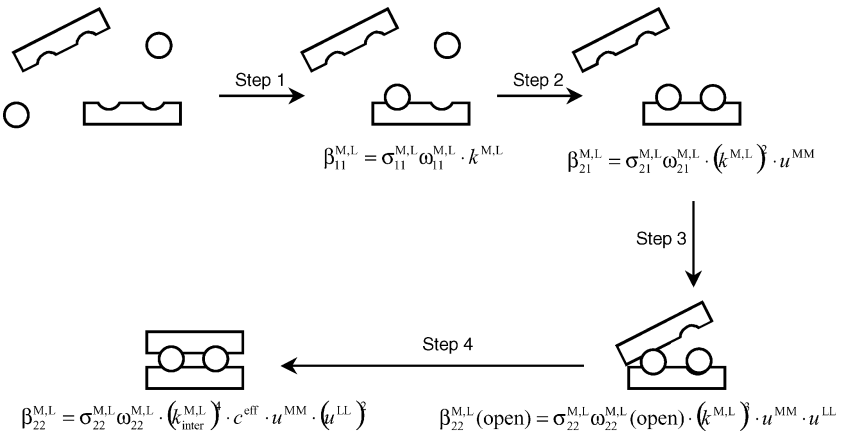

Fig. 17 Schematic formation of the complex $[M_2L_2]$ and its modelling with the extended site binding model (eqn (58)).

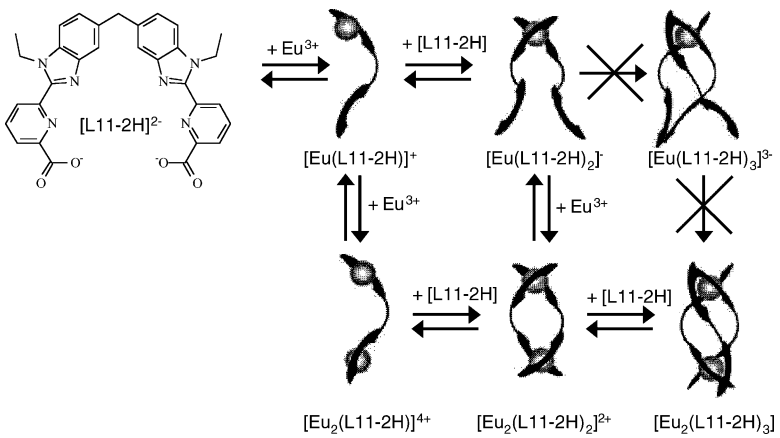

Fig. 18 Schematic representation of the mechanism of the self-assembly of $[Eu_2(L11 - 2H)_3]$. Adapted from ref. 29.

together with ΔE^{MM} and ΔE^{LL} for describing intercomponent interactions in any $[Eu_m(L11 - 2H)_n]^{(3m-2n)+}$ complex produced in equilibria (28′), (29′), (60)–(62). The effective concentration c_i^{eff} is expected to slightly vary with the different levels of preorganization exhibited in the different 'open' complexes undergoing the intramolecular binding process (see step 4 in Fig. 17 for an illustration). According to the limited amount of experimental thermodynamic data, a single average entropic correction c^{eff} is assigned to any intramolecular cyclization in these complexes. Finally, we propose a simple calculation for the degeneracy $\sigma_{chir}^{Eu,L11}\omega_{mn}^{Eu,L11}$ of each microspecies $[Eu_m(L11 - 2H)_n]^{(3m-2n)+}$. Since the free ligands and metals are achiral, $\sigma_{chir}^{Eu,L11} = 1$ except when the point group of the resulting complex does not contain symmetry elements of the second kind (*i.e.* the final complex is chiral), then $\sigma_{chir}^{Eu,L11} = 2$ (Fig. 19). $\omega_{mn}^{Eu,L11} = (C_n^v)^m(C_m^p)^n$ is given by the product of two binomial coefficients, whereby $(C_n^v)^m$ stands for the number of possible arrangements of n ligands connected to v available equivalent positions around each of the m metal ions; v indeed corresponds to the valence of the metal with respect to the denticity of the binding unit, and $v = 3$ when Eu^{3+} is connected to the tridentate binding units of $[L11 - 2H]^{2-}$.[35] Similarly, $(C_m^p)^n$ refers to the number of possible arrangements of m metals connected to p available equivalent positions in each of the n ligands. p indeed corresponds to the total number of binding sites in the ligand, and $p = 2$ for $[L11 - 2H]^{2-}$.[35] The degeneracy calculated for each microspecies is summarized in Fig. 19.

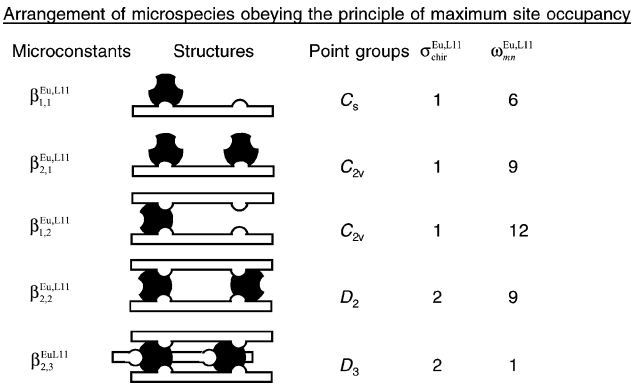

Fig. 19 Schematic structures, symmetries and degeneracies of $[Eu_m(L11 - 2H)_n]^{(3m-2n)+}$ microspecies described in equilibria (28′), (29′), (60)–(62).[35] The point groups are those established in solution (^{1}H NMR, 298 K).

Applying eqn (58) for the formation of $[Eu_m(L11 - 2H)_n]^{(3m-2n)+}$ leads to the global equation (63), which can be detailed for each equilibria (28′), (29′), (60)–(62) to give eqn (64)–(68).

$$\beta_{mn}^{Eu,L11} = \sigma_{chir}^{Eu,L11}\omega_{mn}^{Eu,L11}\left(k^{Eu,L11}\right)^{mn}\left(c^{eff}\right)^{(mn-m-n+1)} \times \left(u^{LL}\right)^{\frac{mn}{2}(n-1)}\left(u^{MM}\right)^{(m-1)} \quad (63)$$

$$\beta_{11}^{Eu,L11} = 6(k^{Eu,L11}) \quad (64)$$

$$\beta_{21}^{Eu,L11} = 9(k^{Eu,L11})^2(u^{MM}) \quad (65)$$

$$\beta_{12}^{Eu,L11} = 12(k^{Eu,L11})^2(u^{LL}) \quad (66)$$

$$\beta_{22}^{Eu,L11} = 18(k^{Eu,L11})^4(u^{LL})^2(u^{MM})(c^{eff}) \quad (67)$$

$$\beta_{23}^{Eu,L11} = 2(k^{Eu,L11})^6(u^{LL})^6(u^{MM})(c^{eff})^2 \quad (68)$$

Table 2 Fitted thermodynamic parameters for $[Eu_m(L11 - 2H)_n]^{(3m-2n)+}$ complexes (water, 298 K, pH = 6.15)[35]

Fitted parameters	$[Eu_m(L11 - 2H)_n]^{(3m-2n)+}$
$\log(k^{Eu,L11})/\Delta g_{inter}^{Eu,L11}$ (kJ mol^{-1})	3.6(1)/−20.8(6)
$\log(u^{LL})/\Delta E^{LL}$ (kJ mol^{-1})	0.9(2)/−5(1)
$\log(u^{MM})/\Delta E^{MM}$ (kJ mol^{-1})	−1.8(3)/10(2)
$\log(c^{eff})/\Delta g_{corr}^{Eu,L11}$ (kJ mol^{-1})	0.3(4)/−2(2)

Standard errors estimated by the least-squares fits are given between parentheses.

A multilinear least-squares fit of eqn (64)–(68) in their logarithmic forms to the experimental macroscopic constants (equilibria (28′), (29′), (60)–(62)) provides the microscopic parameters $\log(k^{Eu,L11})$, c^{eff}, u^{LL} and u^{MM} collected in Table 2.[35] The first parameter $\log(k^{Eu,L11})$ estimates the microscopic free energy balance $\Delta g_{inter}^{Eu,L11} = -21$ kJ mol^{-1} between the partial desolvation of the components and the formation of one intermolecular Eu–(L11 − 2H) connection. The term $\log(c^{eff}) = 0.3$ provides an entropic correction $\Delta g_{corr}^{Eu,L11} = -2$ kJ mol^{-1}, which favours intramolecular cyclization over intermolecular complexation, despite a rather large intersite separation of 9 Å. As expected, $\Delta E^{MM} = 10$ kJ mol^{-1} represents the electrostatic repulsion between two Eu^{3+} occupying two adjacent binding sites. The attractive interligand interaction is more surprising $\Delta E^{LL} = -5$ kJ mol^{-1}, but it can be tentatively assigned to the formation of a stabilizing hydrogen bonding network involving the carboxylate groups brought close together by the complexation process in water.[35]

Since ΔE^{MM} and ΔE^{LL} possess opposite signs, their combination in the global cooperative term ΔE_{dev} (eqn (59)) may induce positive ($\Delta E_{dev} < 0$) or negative ($\Delta E_{dev} > 0$) cooperativity, depending on the structure of the complex under investigation (Table 3). It is

Table 3 Deviation from statistical binding (ΔE_{dev}, eqn (59)) for the formation of the saturated microspecies $[Eu_m(L11 - 2H)_n]^{(3m-2n)+}$

Microspecies	$(mn/2)(n-1)\Delta E^{LL}$	$(m-1)\Delta E^{MM}$	ΔE_{dev}	Cooperativity
$[Eu(L11 - 2H)_2]^-$	−5.1	—	−5.1	Positive
$[Eu_2(L11 - 2H)]^{4+}$	—	10.3	10.3	Negative
$[Eu_2(L11 - 2H)_2]^{2+}$	−9.7	10.3	0.6	Negative (≈none)
$[Eu_2(L11 - 2H)_3]$	−29.7	10.3	−19.4	Positive

Values are given in kJ mol^{-1}.

worth noting that ΔE_{dev} is not a global concept characterizing a complete self-assembly process, but it is defined for each specific complex. For the Eu–L11 system, the formation of the target triple helical complex is eventually driven by positive cooperativity ($\Delta E_{dev} = -19.4$ kJ mol^{-1}), but the formation of intermediates are characterized by negatively cooperative processes (Table 3).

The extended site binding model (eqn (58)) has been further applied to more complicated systems with ligands possessing different binding sites, and long-range intercomponent interaction (*i.e.* more than two metal ions are involved).[34] For instance, the assemblies of the trimetallic helicates $[Cu_3(L2)_2]^{3+}$ (equilibria (1)–(4)) and $[Ln_3(L3)_3]^{9+}$ (equilibria (5)–(7)) have been analyzed with this technique.[34] The main restriction concerns the limited number of experimentally accessible thermodynamic data, which often prevents the least-squares fit of five microscopic parameters, *i.e.* two microscopic affinity for the central k_c and terminal k_t binding sites, two short-range intercomponent interactions ΔE^{LL} and ΔE^{MM} and one entropic correction c^{eff}. For $[Cu_3(L2)_2]^{3+}$, c^{eff} had to be fixed at a reasonable value during the fitting process, and the best results evidence both $\Delta E^{LL} > 0$ and $\Delta E^{MM} > 0$, which implies negative cooperativity for any complexes involved in this assembly process.[34] This result is compatible with repetitive statistical binding demonstrated by using Ercolani's model for this assembly, and simply indicates that fixed repulsive intercomponent interactions affects the successive steps leading to the formation of $[Cu_3(L2)_2]^{3+}$. For the formation of $[Ln_3(L3)_3]^{9+}$, a reinforced negative cooperativity is found ($\Delta E^{LL} > 0$ and $\Delta E^{MM} \gg 0$) because of the higher positive charge borne by the Ln^{3+} cations.

Conclusion and outlook

Since the introduction of a novel semantics borrowed from biology into coordination chemistry during the nineties, major structural achievements have been obtained, but comparatively minor attention has been paid to the related energetical aspects of the self-assembly processes. The original inadequate use of Scatchard plots for the assessment of cooperativity in the self-assembly of multimetallic helicates[15] was easily accepted by the community, then repeated for a decade.[20] It is only recently that the problematic of intra- *vs*. intermolecular connections has been reliably addressed in this field.[21] For being complete, we should mention that Hunter and co-workers, already in 1995,[33c] carefully discussed competition between cyclization and polymerization in metal–ligand self-assembly processes for unravelling aggregation in macrocyclic metalloporphyrins. However, the lack of explicit consideration of metal–ligand complexation processes partially masked the potential of the latter approach for modeling multicomponent complexation processes in coordination chemistry. With the development of the site binding (strictly intermolecular connections) and of the extended site binding (intra- and intermolecular connections) models, simple and quantitative models to assess cooperativity have become available. Moreover, this parametrization of the total free energy of formation opens interesting perspectives for some new predictions concerning the energetics in metallosupramolecular complexes, as illustrated by the recent successful prediction of the stability of the highly charged lanthanide helicate $[Eu_4(L15)_3]^{12+}$ (Fig. 20(a)). In the latter case, the microscopic parameters $k_t^{Eu,L3}$, $k_c^{Eu,L3}$, c^{eff}, u^{EuEu} and u^{LL} previously determined for $[Eu_3(L3)_3]^{9+}$,[34] have been used for

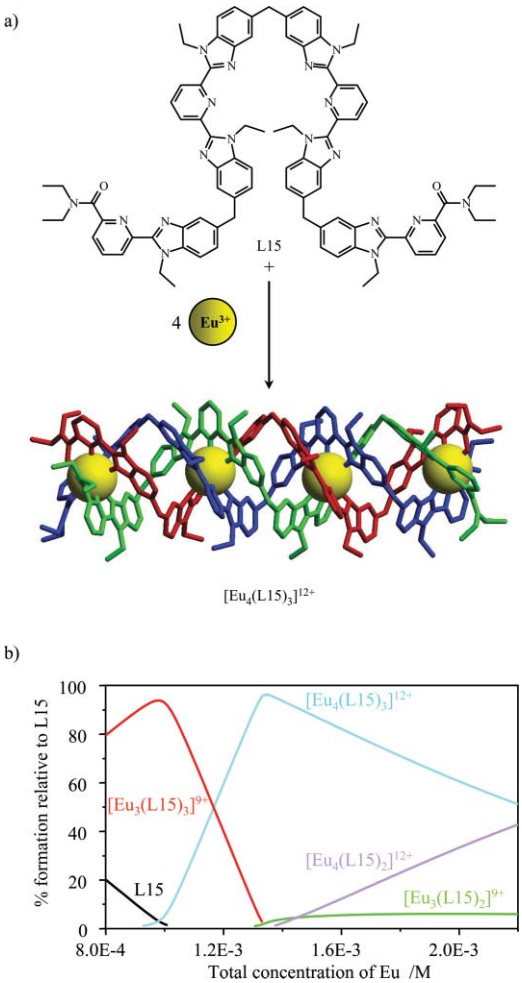

Fig. 20 (a) Formation and molecular structure of $[Eu_4(L15)_3]^{12+}$ (X-ray) and (b) distribution curves predicted for Eu–L15 complexes with $[L15]_{tot} = 10^{-3}$ M.[37]

computing the macroscopic constants shown in equilibria (69)–(72), assuming that L15 contains two central N_3 and two terminal N_2O binding units.[37]

$$3\,Eu^{3+} + 3\,L15 \rightleftharpoons [Eu_3(L15)_3]^{9+}: \log(\beta_{33}^{Eu,L15})_{calc} = 35.5 \quad (69)$$

$$4\,Eu^{3+} + 3\,L15 \rightleftharpoons [Eu_4(L15)_3]^{12+}: \log(\beta_{43}^{Eu,L15})_{calc} = 42.5 \quad (70)$$

$$3\,Eu^{3+} + 2\,L15 \rightleftharpoons [Eu_3(L15)_2]^{9+}: \log(\beta_{32}^{Eu,L15})_{calc} = 27.4 \quad (71)$$

$$4\,Eu^{3+} + 2\,L15 \rightleftharpoons [Eu_4(L15)_2]^{12+}: \log(\beta_{42}^{Eu,L15})_{calc} = 31.5 \quad (72)$$

The associated predicted distribution curves (Fig. 20(b)) show a sufficient domain of stability for $Eu_4(L15)_3]^{12+}$ at millimolar concentration to justify its synthesis. Following this encouraging prediction, L15 has been prepared *via* a complicated multistep strategy (10 steps), and the experimental stability constants with Eu^{3+} were shown to closely match those calculated in equilibria (69)–(72).[37] This shift from parametrization and analysis, toward predictions is obviously not limited to helicates, and any multicomponent assembly is amenable to such treatment. The main limitation concerns the rare occurrence of sophisticated complexation processes, for which complete thermodynamic (and/or kinetic)

characterizations are available. The current craze for reporting short communications with high impact factors mainly drives the attention of talented chemists on aesthetically appealing structural challenges, while the characterization of their formation is often considered as an useless and time-consuming work.

Acknowledgements

Financial support from the Cost Action D31 is gratefully acknowledged.

References

1 J.-M. Lehn, A. Rigault, J. Siegel, J. Harrowfield, B. Chevrier and D. Moras, *Proc. Natl. Acad. Sci. USA*, 1987, **84**, 2565.
2 For reviews, see: (*a*) E. C. Constable, *Tetrahedron*, 1992, **48**, 10013; (*b*) E. C. Constable, *Prog. Inorg. Chem.*, 1994, **42**, 67; (*c*) D. S. Lawrence, T. Jiang and M. Levett, *Chem. Rev.*, 1995, **95**, 2229; (*d*) D. Philp and J. F. Stoddart, *Angew. Chem., Int. Ed. Engl.*, 1996, **35**, 1154; (*e*) C. Piguet, G. Bernardinelli and G. Hopfgartner, *Chem. Rev.*, 1997, **97**, 2005; (*f*) C. Piguet, *J. Inclusion. Phenom. Macrocycl. Chem.*, 1999, **34**, 361; (*g*) D. L. Caulder and K. N. Raymond, *J. Chem. Soc., Dalton Trans.*, 1999, 1185; (*h*) S. Leininger, B. Olenyuk and P. J. Stang, *Chem. Rev.*, 2000, **100**, 853; (*i*) G. F. Swiegers and T. J. Malefetse, *Chem. Rev.*, 2000, **100**, 3483; (*j*) M. Fujita, K. Umemoto, M. Yoshizawa, N. Fujita, T. Kusukawa and K. Biradha, *Chem. Commun.*, 2001, 509; (*k*) G. F. Swiegers and T. J. Malefetse, *J. Inclusion Phenom. Macrocycl. Chem.*, 2001, **40**, 253; (*l*) M. Albrecht, *Chem. Rev.*, 2001, **101**, 3457; (*m*) P. D. Beer and E. J. Hayes, *Coord. Chem. Rev.*, 2003, **240**, 167; (*n*) M. Fujita, M. Tominaga, A. Hori and B. Therrien, *Acc. Chem. Res.*, 2005, **38**, 371.
3 (*a*) A. F. Williams, C. Piguet and R. Carina, *Transition Met. Supramol. Chem.*, 1994, **448**, 409; (*b*) A. F. Williams, R. F. Carina, L. Charbonnière, P. G. Desmartin and C. Piguet, *Nato AST Ser. Phys. Supramol. Chem.*, 1996, 379; (*c*) D. P. Funeriu, J.-M. Lehn, K. M. Fromm and D. Fenske, *Chem. Eur. J.*, 2000, **6**, 2103.
4 X. Sun, D. W. Johnson, D. L. Caulder, K. N. Raymond and E. H. Wong, *J. Am. Chem. Soc.*, 2001, **123**, 2752.
5 (*a*) R. Krämer, J.-M. Lehn and A. Marquis-Rigault, *Proc. Natl. Acad. Sci. USA*, 1993, **90**, 5394; (*b*) J.-M. Lehn and A. V. Eliseev, *Science*, 2001, **291**, 2331.
6 (*a*) J. L. Atwood and L. R. MacGillivray, *Angew. Chem., Int. Ed.*, 1999, **38**, 1018; (*b*) M. Boncheva, D. A. Bruzewicz and G. M. Whitesides, *Pure Appl. Chem.*, 2003, **75**, 621; (*c*) S. Alvarez, *Dalton Trans.*, 2005, 2209.
7 M. Mammen, S.-K. Choi and G. M. Whitesides, *Angew. Chem., Int. Ed.*, 1998, **37**, 2754.
8 J.-M. Lehn and A. Rigault, *Angew. Chem., Int. Ed. Engl.*, 1988, **27**, 1095.
9 J.-M. Lehn, *Supramolecular Chemistry*, VCH, Weinheim–New York–Basel–Cambridge–Tokyo, 1995, p. 142.
10 *Encyclopedia of Supramolecular Chemistry*, ed. J. L. Atwood and J. W. Steed, Marcel Dekker Inc., New York–Basel, 2 volumes, 2004.
11 J. A. Thomas in *Encyclopedia of Supramolecular Chemistry*, ed. J. L. Atwood and J. W. Steed, Marcel Dekker Inc., New York–Basel, vol. 1, 2004, p. 1248.
12 J. S. Lindsey, *New J. Chem.*, 1991, **15**, 153.
13 (*a*) P. J. Stang and B. Olenyuk, *Acc. Chem. Res.*, 1997, **30**, 502; (*b*) P. J. Stang, *Chem. Eur. J.*, 1998, **4**, 19; (*c*) B. Olenyuk, A. Fechtenkötter and P. J. Stang, *J. Chem. Soc., Dalton Trans.*, 1998, 1707.
14 G. F. Swiegers and T. J. Malefetse, *Chem. Eur. J.*, 2001, **7**, 3637.
15 (*a*) T. M. Garrett, U. Koert and J.-M. Lehn, *J. Phys. Org. Chem.*, 1992, **5**, 529; (*b*) A. Pfeil and J.-M. Lehn, *J. Chem. Soc., Chem. Commun.*, 1992, 838.
16 (*a*) K. E. Van Holde, *Physical Biochemistry*, Prentice Hall, Englewood Cliffs, NJ, 2nd edn, 1985; (*b*) B. Perlmutter-Hayman, *Acc. Chem. Res.*, 1986, **19**, 90; (*c*) A. Ben-Naim, *J. Chem. Phys.*, 1998, **108**, 6937.
17 A. V. Hill, *J. Physiol. (London)*, 1910, **4**, 40.
18 G. Scatchard, *Ann. N. Y. Acad. Sci.*, 1949, **51**, 660.
19 R. J. Motekaitis, A. E. Martell and R. A. Hancock, *Coord. Chem. Rev.*, 1994, **133**, 39.
20 S. Floquet, N. Ouali, B. Bocquet, G. Bernardinelli, D. Imbert, J.-C. G. Bünzli, G. Hopfgartner and C. Piguet, *Chem. Eur. J.*, 2003, **9**, 1860.
21 G. Ercolani, *J. Am. Chem. Soc.*, 2003, **125**, 16097.
22 D. L. Caulder and K. N. Raymond, *Angew. Chem., Int. Ed. Engl.*, 1997, **36**, 1440.
23 C. Piguet, M. Borkovec, J. Hamacek and K. Zeckert, *Coord. Chem. Rev.*, 2005, **249**, 705.
24 F. A. Cotton and G. Wilkinson, *Advanced Inorganic Chemistry*, John Wiley & Sons, New York, 4th edn, 1980, p. 70.
25 J. Rydberg, *Acta Chem. Scand.*, 1961, **15**, 1723.
26 J. Wyman, *Q. Rev. Biophys.*, 1968, **1**, 35.
27 G. Koper and M. Borkovec, *J. Phys. Chem. B*, 2001, **105**, 6666.
28 M. Borkovec, J. Hamacek and C. Piguet, *Dalton Trans.*, 2004, 4096.
29 M. Elhabiri, J. Hamacek, J.-C. G. Bünzli and A. M. Albrecht-Gary, *Eur. J. Inorg. Chem.*, 2004, 51.
30 S. Blanc, P. Yakirevich, E. Leize, M. Meyer, J. Libman, A. Van Dorsselaer, A.-M. Albrecht-Gary and A. Shanzer, *J. Am. Chem. Soc.*, 1997, **119**, 4934.
31 (*a*) S. Floquet, N. Ouali, B. Bocquet, G. Bernardinelli, D. Imbert, J.-C. G. Bünzli, G. Hopfgartner and C. Piguet, *Chem. Eur. J.*, 2003, **9**, 1860; (*b*) K. Zeckert, J. Hamacek, J.-P. Rivera, S. Floquet, A. Pinto, M. Borkovec and C. Piguet, *J. Am. Chem. Soc.*, 2004, **126**, 11589.
32 (*a*) D. Chapon, C. Husson, P. Delangle, C. Lebrun and P. J. A. Vottéro, *J. Alloys Compd.*, 2001, **323–324**, 128; (*b*) D. Chapon, J.-P. Morel, P. Delangle, C. Gateau and J. Pécaut, *Dalton Trans.*, 2003, 2745 .
33 (*a*) H. Jacobson and W. H. Stockmayer, *J. Chem. Phys.*, 1950, **18**, 1600; (*b*) W. P. Jencks, *Proc. Natl. Acad. Sci. USA*, 1981, **78**, 4046; (*c*) X. Chi, A. J. Guerin, R. A. Haycock, C. A. Hunter and L. D. Sarson, *J. Chem. Soc., Chem. Commun.*, 1995, 2563; (*d*) L. Mandolini, *Adv. Phys. Org. Chem.*, 1986, **22**, 1; (*e*) R. H. Kramer and J. W. Karpen, *Nature*, 1998, **395**, 710; (*f*) J. M. Gargano, T. Ngo, J. Y. Kim, D. W. K. Acheson and W. J. Lees, *J. Am. Chem. Soc.*, 2001, **123**, 12909; (*g*) P. I. Kitov and D. R. Bundle, *J. Am. Chem. Soc.*, 2003, **125**, 16271. For comprehensive reviews, see; (*h*) M. A. Winnik, *Chem. Rev.*, 1981, **81**, 491; (*i*) G. Ercolani, *J. Phys. Chem. B*, 1998, **102**, 5699; (*j*) C. Galli and L. Mandolini, *Eur. J. Org. Chem.*, 2000, 3117; (*k*) A. Mulder, J. Huskens and D. N. Reinhoudt, *Org. Biomol. Chem.*, 2004, **2**, 3409.
34 J. Hamacek, M. Borkovec and C. Piguet, *Chem. Eur. J.*, 2005, **11**, 5227.
35 J. Hamacek, M. Borkovec and C. Piguet, *Chem. Eur. J.*, 2005, **11**, 5217.
36 M. Elhabiri, R. Scopelliti, J.-C. G. Bünzli and C. Piguet, *J. Am. Chem. Soc.*, 1999, **121**, 10747.
37 K. Zeckert, J. Hamacek, J.-M. Senegas, N. Dalla-Favera, S. Floquet, G. Bernardinelli and C. Piguet, *Angew. Chem., Int. Ed.*, 2005, **44**, 7954.

